

## Article

# Hominid Alluvial Corridor (HAC) of the Guadalquivir and Guadaíra River Valleys (Southern Spain): Geoarchaeological Functionality of the Middle Paleolithic Assemblages during the Upper Pleistocene

Fernando Díaz del Olmo <sup>1</sup>, José A. Caro Gómez <sup>2,\*</sup> , César Borja Barrera <sup>1</sup> , José M. Recio Espejo <sup>3</sup>, Rafael Cámara Artigas <sup>1</sup> and Aránzazu Martínez Aguirre <sup>4</sup>

<sup>1</sup> Department of Geography and A.G.R., University of Sevilla, C/María de Padilla s/n, 41004 Sevilla, Spain; delolmo@us.es (F.D.d.O.); cesarborja@us.es (C.B.B.); rcamara@us.es (R.C.A.)

<sup>2</sup> Department of History, University of Córdoba, Plaza del Cardenal Salazar, 3, 14071 Córdoba, Spain

<sup>3</sup> Department of Ecology, Botany and Plant Physiology, University of Córdoba, Campus de Rabanales s/n, 14071 Córdoba, Spain; bv1reesj@uco.es

<sup>4</sup> Department of Applied Physics I, University of Sevilla, Ctra. Utrera, km 1, 41013 Sevilla, Spain; arancha@us.es

\* Correspondence: jacaro@uco.es

**Abstract:** This research addresses the geomorphological connectivity existing amid the piedmont's karstic fillings (Sierra de Esparteros) and the Guadaíra and Guadalquivir Rivers' alluvial terraces (SW of Spain), spotted with vestiges of human activities (Middle Palaeolithic). This study includes the analysis of 20 geoarchaeological sites and 28 lithic assemblages, with a total of 13,233 lithic pieces. Techno-typological and use-wear (SEM) analyses were conducted on these artifacts. Depending on the raw materials and the provenance of these lithic industries, two groups of assemblages were identified: one made of quartzite from the north, and another made of flint from the south. Two main geochronological periods were established (OSL and U/Th): (1) a short duration (MIS6/MIS5) and (2) a long duration (MIS5/MIS3). Techno-typological analysis showed three sorts of activities: (a) the provision and distribution of raw materials, (b) knapping, and (c) other activities that imply the use of a lithic workshop (LW), along with the settlement characteristics of habitual or recurrent (HS), temporary (TS), and indeterminate (IN). This geoarchaeological connectivity is called the "hominid alluvial corridor" (HAC). The underlined features are the geomorphological units, the continuum alluvial series, the raw material of the lithic industries as an indicator of provenance and transportation throughout the alluvial system, and the use-wear analysis of the tool-kit to interpret the functionality of the pieces.

**Keywords:** Middle Paleolithic; hominid corridor; Upper Pleistocene; use-wear; Guadaíra and Guadalquivir Rivers; Spain



**Citation:** Díaz del Olmo, F.; Caro Gómez, J.A.; Borja Barrera, C.; Recio Espejo, J.M.; Cámara Artigas, R.; Martínez Aguirre, A. Hominid Alluvial Corridor (HAC) of the Guadalquivir and Guadaíra River Valleys (Southern Spain): Geoarchaeological Functionality of the Middle Paleolithic Assemblages during the Upper Pleistocene. *Geosciences* **2023**, *13*, 206. <https://doi.org/10.3390/geosciences13070206>

Academic Editors: Jesús F. Jordá Pardo and Jesus Martinez-Frias

Received: 5 May 2023

Revised: 30 June 2023

Accepted: 3 July 2023

Published: 8 July 2023



**Copyright:** © 2023 by the authors. Licensee MDPI, Basel, Switzerland. This article is an open access article distributed under the terms and conditions of the Creative Commons Attribution (CC BY) license (<https://creativecommons.org/licenses/by/4.0/>).

## 1. Introduction: Alluvial Geoarchaeological Hominid Corridor

Watersheds provide excellent geomorphological connectivity [1]. This connectivity can be categorized into two types: structural and functional. Structural connectivity refers to the connection between adjacent geomorphological units, such as slopes, alluvial terraces, piedmonts, thalwegs, etc. Functional connectivity occurs when there is a linkage between units through hydro-geomorphological processes within and beyond the alluvial floodplain, including features like watershed floods, rill wash, and channel bars [2–4]. These two forms of connectivity facilitated the dispersal of human groups during the Middle Paleolithic, serving as pathways for accessing and stockpiling natural resources. According to Sánchez Hernández et al. [5], Neanderthals in the Mediterranean Iberian Peninsula possessed a comprehensive understanding of the territory. Therefore, the structural connectivity played a significant role and was utilized for Species Distribution Models (SDMs), which

involved statistical modeling of the structural connectivity between Neanderthals and anatomically modern humans (AMHs) to identify optimal habitat patches during the period of 48–40 ka BP. A detailed analysis revealed that the deterioration and reduction of their habitats was primarily attributed to the loss of structural connectivity among these habitat patches rather than solely being a result of climate change. This loss of connectivity was identified as the most crucial factor leading to the extinction of Neanderthals in Europe [6]. The significance of the habitats in the Mediterranean Iberian Peninsula for Neanderthal survival strategies further strengthens this conclusion [5].

Alluvial sediments in watersheds have accumulated with the highest concentration in Middle Paleolithic open-air archaeological sites, some with paleontological remains and some without. We use the term “hominid alluvial geoarchaeological corridor” to describe a watershed that serves as a geomorphological unit with human settlements, which can be occasional, recurrent, or temporary. These settlements may or may not contain fauna remains and have defined functionalities, sometimes complementing each other, such as hunting grounds, butchery practices, and lithic workshops. Additionally, these corridors may contain primary outcrops (geological outcrops) or secondary outcrops (superficial geomorphological formations) that provide high-quality raw materials [7–13]. Therefore, the significance lies in the entire geoarchaeological assemblage within the watershed, rather than specific individual sites. One such landscape with these characteristics can be identified in the Guadalquivir Valley in southern Spain. Here, a Pleistocene sequence of the Guadalquivir River Valley was established, including relative and absolute chronologies (U/Th, OSL), for the Acheulian techno-complexes found in the high and middle terraces (Middle and Upper Pleistocene), as well as for the Middle Paleolithic in the lowest terraces (Upper Pleistocene). This was due to the dispersal of hunter–gatherer groups throughout the watershed [14–23].

This paper specifically focuses on the territorial dispersion at the regional watershed scale, with a particular emphasis on the Guadaíra River watershed [3]. The Guadaíra River is a left bank tributary of the Guadalquivir River, located in the province of Seville, Spain. From a geomorphological perspective, the Guadaíra River provides alluvial connectivity between the limestone and flint outcrops of the Subbetic or Mesozoic–Betic Chain and the middle-lower fluvial terraces of the Guadalquivir River, which contain quartzite pebbles from the Sierra Morena Paleozoic (Figure 1). The interest in this connectivity stems from the fact that both the Guadalquivir and Guadaíra Rivers have Middle/Upper Pleistocene terraces that harbor Middle Paleolithic lithic assemblages, predominantly consisting of quartzite industries from the Guadalquivir River terraces and flint industries from the Guadaíra River terraces. We have termed the geomorphological *continuum* between the karstic piedmont of Sierra de Esparteros (Subbetic Mountains) and the alluvial terraces and colluvial deposits of the Guadaíra and Guadalquivir Rivers as the hominid alluvial corridor (HAC). Within this corridor, the lithic industries made of quartzite and flint are intermixed and dispersed. The HAC is characterized by four key features: (1) the presence of geomorphological units, (2) the continuum of alluvial series, (3) the raw material used in lithic industries as an indicator of provenance and transportation within the alluvial system, and (4) the use–wear analysis of the tool-kit to interpret the functionality of the artifacts.

The main objective of this paper is to define and characterize the HAC from a geoarchaeological and chronocultural perspective. The locations within the HAC exhibit a wide range of geoarchaeological variability, illustrating the geomorphological continuum between the alluvial terraces and the piedmont of the Sierra de Esparteros in Morón de la Frontera, Seville. Within this context, the deposits were interpreted based on the local and regional geomorphological evolution. To enhance the investigation, a physical–chemical characterization and a macro–microscopic analysis of the edges of quartzite flakes were conducted to identify traces of use.

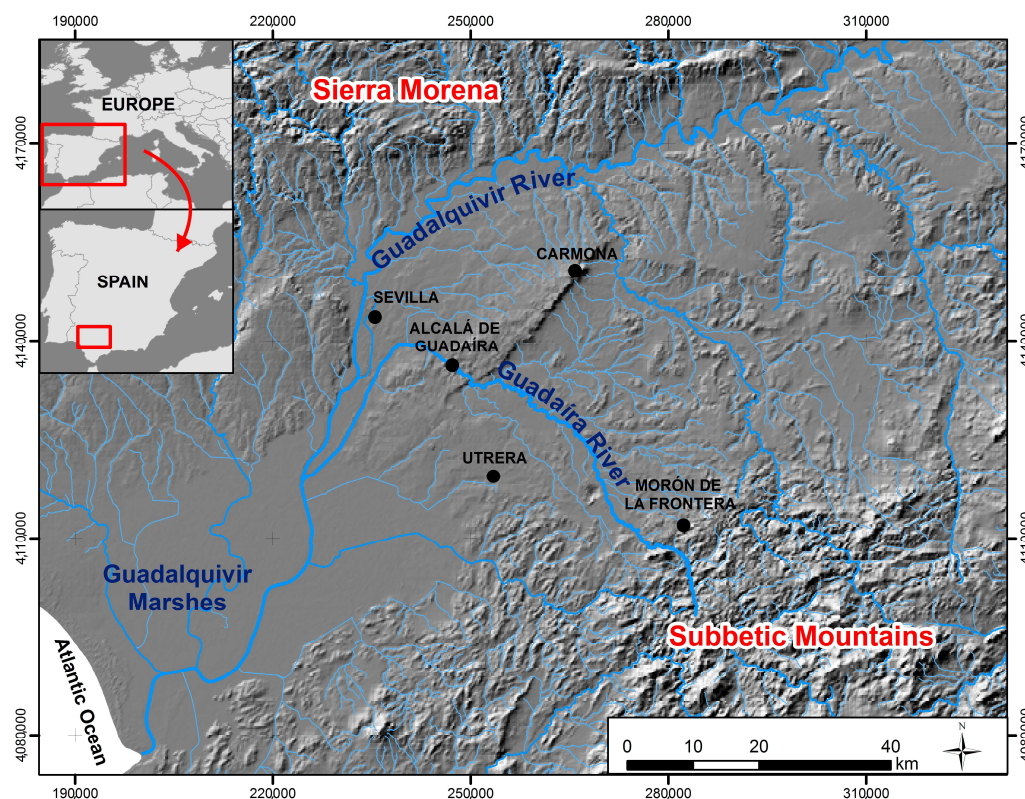


**Figure 1.** Location of studied area.

## 2. Methods

### 2.1. Geoarchaeological Field Work

Geomorphological transects were conducted in the sediments of the Middle–Upper Pleistocene Guadaíra watershed, spanning from the Subbetic Mountains to the alluvial connection with the Guadalquivir River. Four cross-sections were implemented for this geomorphological analysis, namely the karstic piedmont–Sierra de Esparteros, Upper Guadaíra–Balbuan, Middle Guadaíra–Rozalejo, and Low Guadaíra–Barranca–Marchenilla–Membrilla–La Liebre. In the Guadalquivir River, the T11 (+44 m) and T12 (+28 m) terraces connected to the Guadaíra River and the geomorphological surface deposits from the T6 to T10 terraces were studied. Throughout these areas, a total of 20 geoarchaeological sites (with 28 lithic assemblages) were identified. These sites are associated with industries found in the alluvial sediments of the Guadalquivir, Guadaíra, and Rozalejo rivers, the karstic fillings of the Sierra de Esparteros piedmont (Cerro Santisteban), the colluvial deposits in Rozalejo and La Liebre, and the geomorphological surface deposits (Figure 2; Table 1).

The alluvial and colluvial deposits are correlated with the entire Middle–Upper Pleistocene alluvial terraces in the Guadalquivir River [14,22–24]. Based on the provenance of the raw materials used in the pebble industries, two distinct groups have been identified: quartzites from the north and flint from the south. As for the nomenclature of the fluvial terraces, we have maintained our customary classification, which is based on the morphogenesis and morphotopographic position, ranging from T1 (the oldest terrace) to T14 (the most recent) [25]. Laboratory methods were employed for particle size distribution using the Soils Survey England and Wales guidelines [26], total carbonates analysis [27], and color assessment using the Munsell Color system [28].

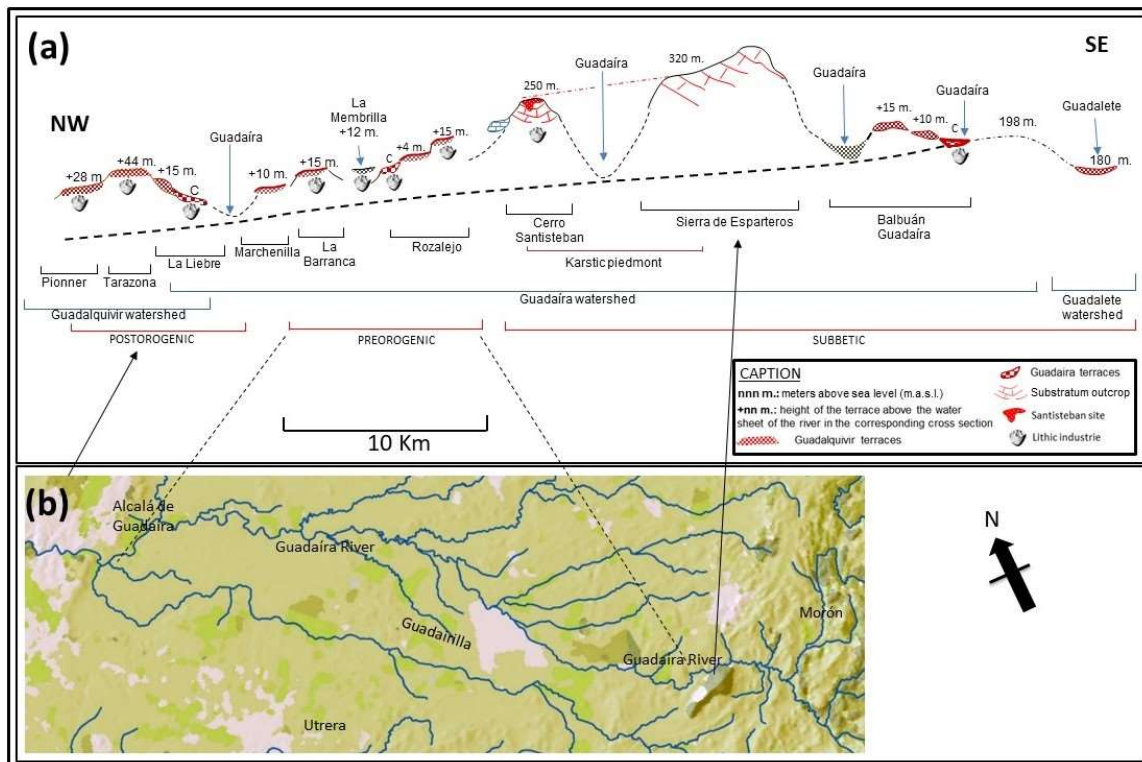


**Figure 2.** Geomorphological profile of the Middle–Upper Pleistocene sediments in the Guadaira River basin, between Sierra Subbética and the alluvial connection with the Guadalquivir River (a) and its cartographic correspondence (b).

## 2.2. Lithic Industries: Techno-Typological Analysis, Traceology Protocol, and Use-Wear

The lithic industries recovered from TAR-II, TAR-III, MUH-4, SAL-2, CAS-1, PIO (1, 2, 3, and 4), AER-2, REY (1 and 3), PIL-1, MOL-1, MAJ-1, CORT-1, CAL-1, TOR-3, PAD-1, BAR-1, MEM-1, LIE-1, ROZ-1, and SAN-1 (Table 1) were typologically characterized, following the frameworks of Bordes [29], Tixier [30], Clark [31], Boëda et al. [32,33], and Caro [21,34]. The analysis included a technological examination of the assemblages to identify operative schemes and retouched pieces. The cores were analyzed based on three criteria: (1) the number, distribution, and hierarchy of extractions; (2) the number of flaking planes; and (3) the quantity and typology of percussion planes. Four parameters were utilized to assign the industry to a mode, including the ratio between flake tools and flakes, the variability of types of flakes, the variability and complexity of operative chains, and the proportion of large tools (presence/absence and variability factors, primarily of biface tools) [16,31,35–44].

In terms of morphometric analysis, two elements were considered: first, a comparison between the size and lithology of the raw material to assess the selection processes, and second, the categorization of the rounded lithic industries (R) into four categories: R0 (unrounded), R1 (slightly rounded), R2 (moderately rounded), and R3 (very rounded) [21,34].

Furthermore, a techno-typological analysis was conducted, following a traceology protocol applied to quartzite notches, consisting of three steps [45]: (1) use–wear analysis of the lithic pieces; (2) analysis on a binocular microscopic scale using equipment such as the Wild Heerbrugg and the Leica DMLM at the Department of Physical Geography, University of Seville; and (3) gold metallization (Sputtering, EDWARDS, Scancoat-Six) and scanning electron microscope (SEM) analysis (Jeol 6460LV) at CITIUS, Microscopy Service, University of Seville, Spain, with the magnification ranging from 100 to 1000 times. The use–wear analysis involved studying micro-traces related to the main features, such as polish, rounding, striation, or ridge concavities. Additionally, an experimental analysis was conducted.

**Table 1.** Location and main characteristics of the archaeological sites analyzed: location; archaeological site; terrace level; deposit; number of pieces; raw material (Qt, quartzite; F, flint; Qz, quartz; O, others); rounded (R0, unrounded; R1, slightly rounded; R2, moderately rounded; R3, very rounded).

Location	Archaeological Site	Terrace Level	Deposit	Pieces n°	Raw Material (%)				Rounded			
					Qt	F	Qz	O	R0	R1	R2	R3
GUADALQUIVIR RIVER	TAR-II	T11	Loam-clay	2885	72	25	2	1	95	5	0	0
	TARIII-1	T11	Gravel bars	264	92	5	2	1	99	1	0	0
	TARIII-2	T11	Loam-clay	118	94	2	3	1	95	5	0	0
	TARIII-3	T11	Gravel and sand bars	727	95	3	1	1	95	5	0	0
	TARIII-4	T11	Gravel bars	1275	85	2	5	8	60	30	9	1
	TARIII-5	T11	Floating gravels	25	84	4	8	4	95	5	0	0
	MUH-4	T7	Loam-clay	273	92	7	1	0	96	4	0	0
	SAL-2	T10	Loam-clay	312	78	20	0	2	81	17	2	0
	CAS-1	T10	Geomorph. surface	330	89	10	0	1	85	14	1	0
	PIO-1	T12	Gravel bars	62	70	25	0	5	11	27	51	11
	PIO-2	T12	Gravel and sand bars	222	74	22	2	2	7	37	38	18
	PIO-3	T12	Gravel and sand bars	108	48	50	0	2	17	43	31	9
	PIO-4	T12	Loam-clay	54	92	8	0	0	90	4	6	0
	AER-2	T12	Loam-clay	45	78	22	0	0	16	84	0	0
	REY-1	T12	Gravel bars	27	99	1	0	0	0	7	27	64
	REY-3	T12	Loam-clay	128	90	9	0	1	58	40	2	0
	PIL-1	T9	Geomorph. surface	590	91	7	1	1	91	8	1	0
	MOL-1	T9	Geomorph. surface	2159	94	5	0	1	4	92	4	0
	MAJ-1	T6	Geomorph. surface	195	99	1	0	0	0	58	37	5
	COR-1	T6	Geomorph. surface	222	98	1,5	0	0,5	0	54	44	2
CAL-1	T8	Geomorph. surface	91	90	9	0	1	20	79	1	0	
TOR-3	T7	Geomorph. surface	190	85	12	1	2	94	6	0	0	
PAD-1	T7	Geomorph. surface	950	93	6	0	1	14	51	28	7	
GUADAIIRA RIVER	BAR-1		Geomorph. surface	44	75	23	2	0	75	25	0	0
	MEM-1	T (+10)	Gravels and fine grav.	3	0	100	0	0	100	0	0	0
	LIE-1		Geomorph. surface	45	96	2	0	0	100	0	0	0
	ROZ-1	Coll/alluv	Geomorph. surface	208	18	80	0	2	100	0	0	0
KARSTIC PIEDMONT	SAN-1		Karst detrial fill	1656	2	92	0	6	100	0	0	0

### 2.3. Functionality Criteria of the Archaeological Sites

To interpret the functionality of the archaeological sites as part of the HAC, two sets of criteria were employed. The first set focused on the operative chain, considering the technological aspects, such as the breadth and balance of the series, the dimensions and composition of the artifacts, the presence or absence of knapping remains, and the abundance of retouched tools. The second set of criteria pertained to taphonomic features, including the type of deposit, the lithic rounded index, etc.

Based on these criteria, four categories of functionality were established: (HS) habitual or recurrent site, (TS) temporary site, (LW) lithic workshop, and (IN) indeterminate. However, this paper does not address subsistence strategies [46–48], as fauna remains were only found in the detrital fill site of the Cerro Santisteban karst, and they have not yet undergone stratigraphic analysis. Similarly, the Pioneer (PIO) site exhibits displaced fauna remains (*Equus* sp., *Bos* sp., etc.) that have not been thoroughly studied.

#### 2.4. Chronological Framework

The chronological framework was established using optically stimulated luminescence (OSL) and uranium–thorium (U/Th) dating techniques conducted by two different laboratories: the Laboratorio de Datación Radioquímica (LDR) at the Autonomous University of Madrid, and the Laboratorio de Física Aplicada I at the University of Seville, both located in Spain.

The Tarazona III chronologies are based on chronological analysis using OSL dates, which were previously published [22]. On the contrary, the samplings from La Barranca and Marchenilla were studied for the first time in this study.

OSL dating and the additive dose method were carried out in order to determine the time elapsed since the last exposure to sunlight of the sediments. The samples were subjected to a previous anomalous decay test; this study was carried out from the OSL response (TL-DA-10 system) obtained from the samples in a second scan, after being stored in the dark for a period of time of 600 h. Thus, when the detected signal losses were less than 3%, the test was considered negative, and the possible anomalous decay phenomenon was insignificant.

The signal losses detected in the samples studied were always less than 1%. Based on these results, the selected dating method was the fine-grained one [49], consisting of a selection of the mineral fraction with a grain size between 2 and 10 microns.

The total dose stored by each sample since it underwent its last solar bleaching process (equivalent dose) was evaluated by the additive dose method. Increasing doses were supplied by a Sr-Y90 source with a dose rate of 0.0404 Gy/sec. In order to determine a possible supralinear behavior, a second scan was carried out, with small beta doses [50]. The effectiveness of the alpha particles in producing OSL (K factor) was determined by delivering increasing alpha doses using an Am<sup>241</sup> source, with a dose rate of 0.0297 Gy/sg.

The annual doses received by the samples were calculated by combining two types of measurements, including the determination of the beta radioactivity from the K-40 present in the samples using a Geiger–Müller counting system and the measurement of alpha activity from uranium and thorium, also present in the samples, in this case, using a solid scintillation (ZnS) counting system. In the latter method, no activity losses were observed as a consequence of possible radon leaks. The gamma activity from cosmic radiation was measured in situ during the sampling by means of an INa(TL) solid scintillation counting system. Conversions of the alpha, beta, and cosmic count rates to the dose rate were made based on studies by Nambi and Aitken [51].

The errors associated with the estimated ages took into account both the systematic and statistical errors corresponding to the OSL measurements, established dose rates, and calibration processes of the radioactive sources and equipment used [52,53].

U/Th analyses were conducted on the sediments filling the Cerro Santisteban site. Specifically, ten samples of bones and teeth, as well as two samples of carbonated sediments from palustrine facies, were studied. The sample treatment involved dissolving 1 to 5 g of a bone or tooth sample in concentrated nitric acid. Known amounts of <sup>232</sup>U and <sup>229</sup>Th were added to the solutions prior to the precipitation of Fe hydroxides, along with U and Th isotopes. The precipitate was then dissolved in HCl, and controlled precipitation to pH 2.5–3.0 was carried out to separate P and U from Th. A solvent extraction method using TBP and xylene was employed to further separate P from U and Fe from Th. Finally, both elements underwent additional purification using anion exchange resin (Dowex AG1-X8). The purified samples were electro-deposited on stainless steel discs and measured

using alpha spectrometry. The results of the analyses indicate isotopic equilibrium in all the samples, suggesting consistency with the obtained isotopic data and providing a chronology ranging from the Late–Middle Pleistocene to the Upper Pleistocene.

### 3. Results

#### 3.1. Guadaíra Watershed: Distribution of Archaeological Sites with Lithic Industries per Geomorphological Units

The alluvial terrace system of the Guadaíra River is located between the Subbetic karstic piedmont and the T12 terrace level of the Guadalquivir River, which is situated at an elevation of +26 to +29 m.

##### 3.1.1. Karstic Piedmont of the Sierra de Esparteros and Cerro Santisteban

Among the limestone formations on the northern slope of the Sierra de Esparteros and within the Guadaíra watershed, remnants of a karstic piedmont can be observed at an approximate elevation of 320 m. This piedmont has undergone erosion and dissection due to the fluvial activity of the Guadaíra River and its tributaries, such as the Rozalejo River. The limestone outcrops are situated at a higher morphotopographic position, forming a prominent hill known as Cerro Santisteban (250 m). This hill is composed of oolitic limestones and displays a karstified piedmont surface. The ridges of Cerro Santisteban exhibit an epikarst layer, with an underlying sequence of detrital fill referred to as SAN-1 (Figure 3). The detrital deposit in SAN-1 reveals a lower section (level 2.1, Table 2) comprising silt, sand, limestone fragments, and flint clasts. In the upper part (level 2.2, Table 2), a brecciated conglomerate is present, consisting of clasts, lithic industries, herbivorous bones, and teeth. The isotopic dating of carbonate samples from bones and teeth yielded a chronology ranging from  $135.5 \pm 9.9$  ka to  $74.8 \pm 13.2$  ka BP (U/Th) (Table 3).

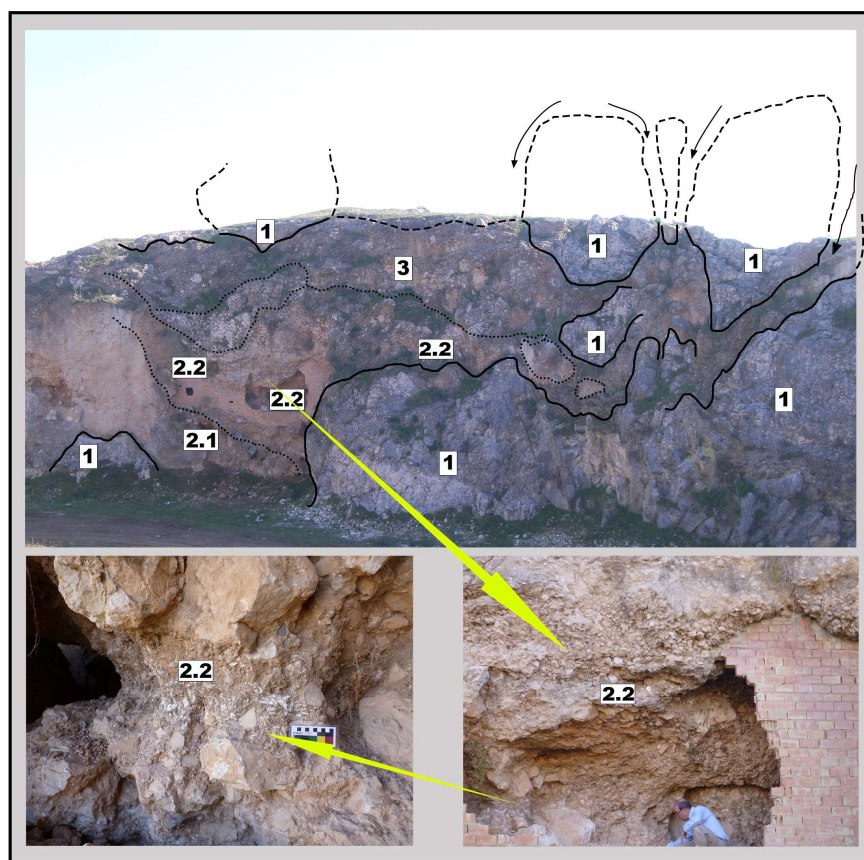


**Figure 3.** Cerro Santisteban’s stratigraphic levels description: (1) substratum outcrop; (2.1) detrital fill (silt, sand–limestone, and flint clasts); (2.2) detrital fill (brecciated conglomerate, clast; herbivorous teeth and bones; lithic industry); (3) breccia (clasts and stone blocks).

**Table 2.** Cerro Santisteban’s stratigraphic levels description (elements and chronologies).

Site	Stratigraphical Levels and Processes	Particle Size Distribution Blue: Sands Red: Silt-Clay	Munsell Colour	CO <sub>3</sub> <sup>=</sup> %	Lithology	Chronology U/Th	Industry	
Cerro Santisteban: karstic piedmond	5.- Pedogenesis		10YR 5/3 7.5YR 4/4 7.5YR 4/6	-				
	4.- Palustrine carbonates.		7.5YR 7/6	76		69.8 ± 2.7 ka 71.7 ± 3.7 ka		
	Karstification episode							
	3.- Breccia (clast and stone block)							
	2.2.- Detrital fill (brecciated conglomerate, clast; herbivorous teeth and bones)		10YR 4/3 10YR 4/4	50 0	Limestone Flint	74.8 ± 13.2 ka 78.2 ± 5.5 ka 87.3 ± 3.9 ka 88.9 ± 5.9 ka 99.9 ± 21.2 ka 100.9 ± 15.3 ka 114.2 ± 10.5 ka 123.6 ± 7.1 ka 135.5 ± 9.9 ka 136.4 ± 18.1 ka	Middle Palaeolithic	
	2.1.- Detrital fill (silt, sand and limestone and flint clasts).		10YR 6/2 7.5YR 8/4	56 90	Limestone Flint			
1.- Substrate outcrop								

**Table 3.** Santisteban's U/Th results and chronologies. All bones and the tooth were dated using the early uptake model. No diacritical corrections were made in any of the samples. The  $^{234}\text{U}/^{238}\text{U}$  activity ratio in the last column is the activity ratio between both uranium isotopes at the initial time.

Sample	$^{238}\text{U}$	$^{234}\text{U}$	$^{234}\text{U}/^{238}\text{U}$	$^{230}\text{Th}$	$^{230}\text{Th}/^{234}\text{U}$	$^{230}\text{Th}/^{232}\text{Th}$	T (ky)	$^{234}\text{U}/^{238}\text{U}$
G2.1-1	15.36 ± 0.32	17.23 ± 0.34	1.122 ± 0.025	9.64 ± 0.21	0.559 ± 0.017	80 ± 12	87.3 ± 3.9	1.155 ± 0.033
G2.1-2	13.03 ± 0.35	14.55 ± 0.38	1.117 ± 0.036	8.23 ± 0.29	0.566 ± 0.025	56.7 ± 11.3	88.9 ± 5.9	1.149 ± 0.046
G2.2-1	14.49 ± 0.31	17.25 ± 0.34	1.191 ± 0.028	12.02 ± 0.30	0.697 ± 0.022	89 ± 17	123.6 ± 7.1	1.270 ± 0.040
G2.2-2	13.22 ± 0.29	15.75 ± 0.33	1.192 ± 0.028	11.53 ± 0.37	0.733 ± 0.028	26.1 ± 3.6	135.5 ± 9.9	1.280 ± 0.041
G2.3-1	2.567 ± 0.071	3.147 ± 0.081	1.226 ± 0.042	1.939 ± 0.252	0.616 ± 0.082	20.7 ± 9.6	99.9 ± 21.2	1.299 ± 0.056
G2.3-2	2.560 ± 0.072	3.108 ± 0.081	1.214 ± 0.041	2.290 ± 0.147	0.737 ± 0.051	12.7 ± 2.5	136.4 ± 18.1	1.313 ± 0.060
G2.4-1	2.005 ± 0.047	2.478 ± 0.053	1.236 ± 0.034	1.658 ± 0.082	0.669 ± 0.036	13.1 ± 2.2	114.2 ± 10.5	1.324 ± 0.047
G2.4-thooth	1.147 ± 0.040	1.402 ± 0.044	1.223 ± 0.054	0.869 ± 0.078	0.620 ± 0.059	96.1 ± 56.1	100.9 ± 15.3	1.296 ± 0.072
G2.5-1	3.478 ± 0.083	3.942 ± 0.089	1.133 ± 0.033	1.986 ± 0.241	0.504 ± 0.062	23.7 ± 10.9	74.8 ± 13.2	1.164 ± 0.040
G2.5-2	2.875 ± 0.061	3.434 ± 0.069	1.194 ± 0.029	1.793 ± 0.081	0.522 ± 0.026	15.2 ± 2.5	78.2 ± 5.5	1.242 ± 0.036
W1.CR2-1	2.387 ± 0.045	2.825 ± 0.052	1.184 ± 0.014	1.360 ± 0.029	0.481 ± 0.014	25.8 ± 1.7	69.8 ± 2.7	1.223 ± 0.017
<b>W1.CR2-2</b>	<b>2.464 ± 0.047</b>	<b>2.879 ± 0.054</b>	<b>1.168 ± 0.014</b>	<b>1.411 ± 0.044</b>	<b>0.490 ± 0.018</b>	<b>24.2 ± 2.2</b>	<b>71.7 ± 3.7</b>	<b>1.206 ± 0.017</b>

From level 2.2, a substantial collection of lithic industries (1,656 pieces) was recovered from SAN-1. These industries mainly comprise knapped products, such as flakes and tools, exhibiting remarkable morphological and technological homogeneity [54]. Typological analysis revealed that the majority of the elements are medium to small in size, with a notable presence of non-cortical and fine products featuring triangular outlines and faceted butts. These products are predominantly the result of a knapping technique demonstrating a centripetal tendency similar to Levallois (*paralevallois sic.*) [46]. The series primarily consists of flint (92%), with minor proportions of limestone (6%) and other raw materials (quartzite 2%). The key characteristics of the assemblage include (a) the absence of bifacial tools; (b) the predominance of Group II artifacts with a high index (63), along with significant occurrences of Levallois (13) and Group III (9), while denticulate and notched specimens are less represented (2 and 3, respectively); (c) the prevalence of simple retouching, both marginal and deep, occasionally exhibiting stepped retouch; (d) a technical Levallois index (Li 19) and a high value of transformation index (50); (e) pronounced faceting index (Fi 50); (f) noticeable technical imbalance due to the scarcity of cores, although other elements of the operative chain (including flakes and small knapping debris) are well-represented. The detrital fill is capped by successive levels devoid of lithic industries, consisting of a breccia deposit (level 3) and a karstification episode. This was followed by the development of a palustrine carbonate facies (level 4), with isotopic dating indicating a chronology ranging from  $71.7 \pm 3.7$  ka to  $69.8 \pm 2.7$  ka BP (U/Th) with an acceptable isotopic  $^{230}\text{Th}/^{232}\text{Th}$  ratio (W1.CR2 sample) (Table 3). Lastly, a pedogenesis period (level 5) occurred subsequently following the carbonate facies.

### 3.1.2. Guadaíra Alluvial Corridor: Three Geomorphological Transects

Three sectors were analyzed within the area encompassing the Guadaíra alluvial corridor:

#### 1. Balbuan terraces: Upper Guadaíra cross-section

In this section, the river presents a narrow alluvial valley modeled mainly over the Trias-Keuper gypsum marl. Morphotopographically, it exposes a complex of two stepped terraces and one colluvial deposit topographically lower than the terraces that connect to the Guadaíra alluvial plain. Different areas were recognized:

- (a) High terrace (+15 m): Eroded above, this is a conglomerate deposit with a 4 m maximum thickness, consisting of subangular to subrounded blocks, pebble, and fine-gravel, with a partially crusted carbonated matrix of medium to coarse sand and a planar structure. Lithologically, there is a predominance of sandstones and limestones, accompanied by ophites and flints. In the interior of the deposit, no lithic industries have been found, but on its geomorphological surface, some lithic elements of untumbled flint (cores and flakes) have been collected, although their scarcity and decontextualization make impossible any techno-typological characterization.
- (b) Lower terrace (+10 m): This terrace has also experienced erosion and exhibits a visible maximum thickness of 3 m. It comprises a deposit of pebbles and fine gravel with an abundant sandy-loam matrix. At the base, the deposit becomes more conglomeratic and channeled, while the top exhibits a planar structure. The lithology observed in this terrace is consistent with that of the upper terrace. No lithic industries have been identified within this alluvial terrace.
- (c) Colluvial-alluvial deposit: This deposit, with a maximum thickness of 1 m, overlays the current floodplain. It possesses a detrital nature, characterized by an abundant sandy-loam matrix. The base of the deposit shows channeling, and scattered pebbles and fine gravel can be found throughout. The lithology of this deposit is similar to that observed in the previous terraces. Some fragments of knapped flint have been recovered from the interior of this deposit.

#### 2. Rozalejo River terraces: middle Guadaíra cross-section

The Rozalejo River, located on the right bank of the Guadaíra River, is a tributary that exhibits a wide valley with several significant features:

- (a) High alluvial deposits (+15 m): These deposits consist of subangular gravel composed of limestone, sandstone, and flint, embedded in a reddish-brown sandy matrix. On the surface deposit in the Pintado Bajo area, unrounded lithic remnants made of flint and quartzite (cores and flakes) have been found. However, these remnants do not possess any specific techno-cultural characterization. It is worth noting that the presence of quartzite stones, including knapped ones and pebbles, in the Guadaíra watershed, where quartzite geological outcrops are absent, suggests deliberate human intention. This indicates that the raw material and lithic tools were brought from the Guadalquivir watershed to the Guadaíra River.
- (b) Alluvial deposit (+4 m): This deposit comprises gravel with similar characteristics to the previous one, but no lithic tools have been discovered.
- (c) Colluvial–alluvial deposit: This deposit is situated on reddish-brown sand and forms a superficial cover of gravel, which connects to the higher topographies of the stream’s right bank. Within this layer of gravel, a collection of 226 lithic artifacts was obtained, including 60 cores, 98 flakes, and 68 utensils (Figure 4). A total of 81% of these artifacts were knapped from various flint materials, 16% from quartzites, and the remaining 3% from sandstone and other raw materials. Most of the artifacts exhibit no alluvial rounding (R0) and have retained their sharp edges, except for a few instances that show slight edge softening possibly caused by water action (R1). Among the different types of cores, simple cores were the most prominent, with 32 examples, followed by centripetal cores (7), Levallois pieces (5), and a total of 7 polyhedral and prismatic pieces (with an additional 9 finished pieces).

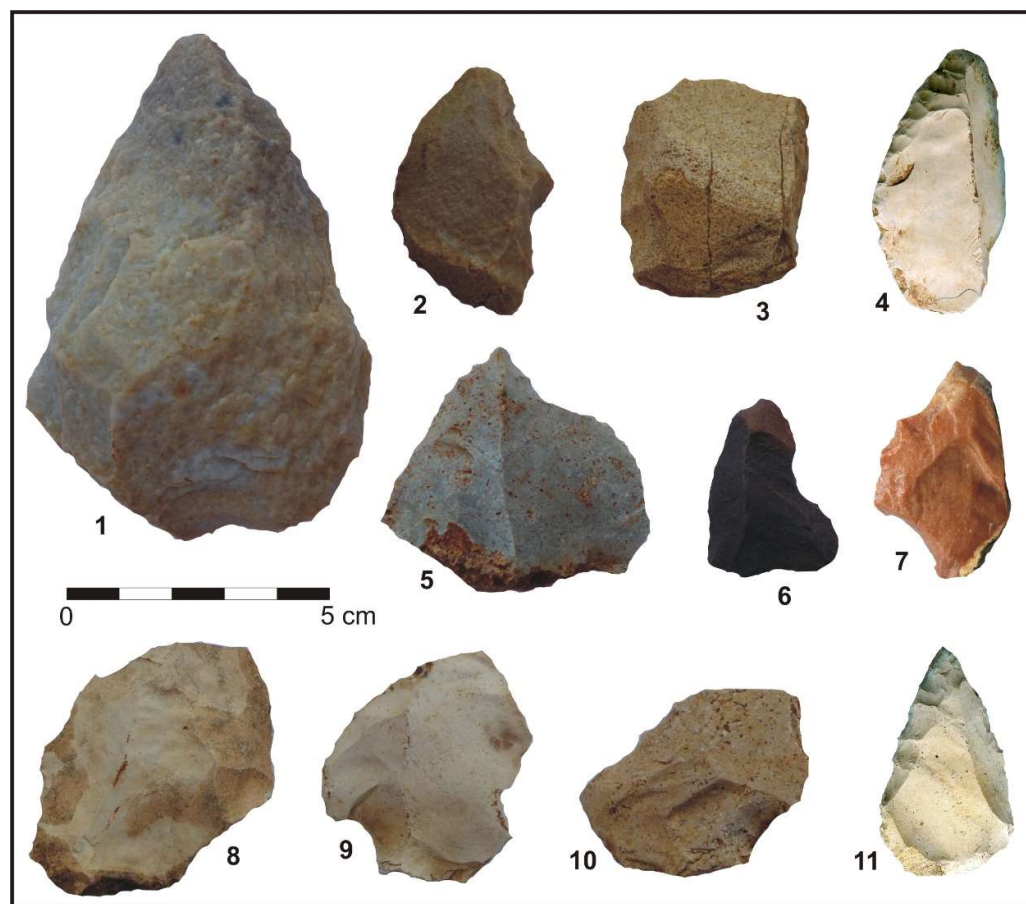


**Figure 4.** Rozalejo (ROZ-1) lithic industry: handaxe (1); scrapers (2, 3, and 4); borer (5); notch (6); denticulate (7); Levallois flakes (8, 9, and 10); Mousterian point (11). Raw materials: quartzites (1, 2, and 6); flint (3, 4, 5, 7, 8, 9, 10, and 11).

The average size of the artifacts differs between those made of flint (55 × 45 mm) and those made of quartzite, with the latter being slightly larger (60 × 60 mm). Internal flakes constitute 62.3% of the total, while cortical flakes account for 16.3%, and subcortical flakes make up 21.4%. The largest dimensions observed were 70 × 40 mm, but smaller flakes below 10 mm were also recovered, with the average size typically around 40 × 30 mm.

Among the 68 utensils, the following typologies have been identified: 18 scrapers, predominantly simple, although one exhibits bifacial characteristics with a simple and shallow finishing; 4 denticulates that are relatively less worked; 6 atypical end-scrapers with one-sided finishing; 6 flakes with finished margins; 11 simple notches; 2 atypical borers; 1 burin made from a large quartzite flake; 1 broken Levallois point; 17 Levallois flakes; 1 Mousterian point with a deeply scaled finishing; 1 subcordiform handaxe made of quartzite; and 6 different tools with a denticulated finishing.

Regarding the butt types, plain butts are the most prevalent (49.5%), followed by cortical butts (24.2%) and depressed butts (13.1%). Faceted butts are also present (12.1%), along with one dihedral butt (1%). Among the simple cortical flakes, they represent 32%, while faceted flakes make up 4%. However, in the category of flake tools, the percentage of faceted versions increases to 25%, while cortical decreases to 8%, and plain flakes rise to 60%.

(d) A deposit of large reddish-brown sand without gravel was found in discordance with the underlying marl substratum.

3. La Barranca, Marchenilla, Membrilla, and La Liebre terraces: low Guadaíra cross-section

The middle and lower terraces of the Guadaíra are situated in the Guadalquivir sedimentary basin, north of the Subbetic limestone outcrops, in both the pre- and post-orogenic periods. These terraces are well-defined in the La Barranca and Marchenilla sites. The higher terrace is located at +12/+10 m, with a maximum thickness of 4–5 m, and exhibits continuous presence along the left bank. The lower terrace is found at +10/+7 m.

In the La Barranca section, two major alluvial episodes can be distinguished. The upper alluvial terrace (+15 m) consists of a sandy-loam deposit with pedological carbonates and hydromorphic soil conditions at the top [27]. No lithic industry has been found within this deposit. However, at the geomorphological surface, in association with these colored soils (10 YR), a series of 44 pieces (BAR-1) was collected. These include 15 simple flake tools, 2 remains of knapping, and 6 with possible use-wear. Additionally, there are 9 cores and 18 tools. Quartzite is the predominant raw material (75%), followed by flint (23%), and other materials, such as sandstone or quartz (2%). Internal flakes are the most common (82%), with the rest being semi-cortical (18%). Among the recognizable butts, the majority are cortical and smooth (70%), while 2 are faceted (10%), and a high number are unrecognizable (20%). Simple cores are the most prevalent, with various extractions from a single plane of percussion, along with centripetal cores (usually with some peripheral preparation), represented by four examples each. The lithic pieces are mostly small-sized (<50 mm), showing signs of numerous extractions and near exhaustion. Notably, there are scrapers among the flake utensils, including simple, flat-surfaced, triple-convergent, and transversal types, exhibiting fine examples of simple-scaled and deep finishing. Other findings include one Levallois point, one Levallois flake tool, one typical scraper, one Mousterian flint point, one burin, one notch, one denticulate, and two diverse tools. Group II is predominant (I = 52), with an acceptable representation of Group I Levallois (I = 11), indicating a technical index of 20 and a transformation rate of 60. The lower terrace (+10 m) consists of an alluvial deposit composed of gravels and fine gravels (sandstone, limestone, and flint), partially rounded to rounded. The top layers alternate with sand. The sandy layer was dated to approximately  $48,860 \pm 3168$  years BP using OSL dating (Table 4).

**Table 4.** Marchenilla, La Barranca, and Tarazona OSL chronologies results (LDR, laboratory).

Field Samples	LDR * Samples	Level	Grain Size ( $\mu$ )	Radionuclide Concentrations					Equivalent Dose (Gy)	Annual Doce (mGy/year)	Factor K	Age (BP)	References
				U (ppm)	Th (ppm)	K <sub>2</sub> O (%)	H <sub>2</sub> O (%)	H <sub>2</sub> O Sat (%)					
<b>GUA-II</b>	MAD-145SDA	Level 5	2–10	0.93	1.811	0.05	9.21	-	80.69	0.78	0.05	10,3448 $\pm$ 7984	
<b>TG1-C</b>	MAD-5791rBIN	Level 1	2–10	0.82	2.63	0.03	8.42	-	56.19	1.15	0.11	48,860 $\pm$ 3168	
<b>TCR-1</b>	MAD-5756rBIN	Level 4	2–10	1.53	9.51	0.13	13.09	13.09	155.39	1.48	0.10	104,993 $\pm$ 8415	Caro et al., 2011 [22]
<b>TCR-2</b>	MAD-5757rBIN	Level 6	2–10	2.02	7.47	0.73	8.60	8.60	195.25	1.77	0.08	110,310 $\pm$ 10,290	Caro et al., 2011 [22]
<b>TCR-3</b>	MAD-5763rBIN	Level 8	2–10	2.71	6.19	1.22	8.12	8.12	283.50	2.33	0.09	121,673 $\pm$ 9837	Caro et al., 2011 [22]
<b>TCR-4</b>	MAD-5761rBIN	Level 8	2–10	2.36	6.64	0.48	8.41	8.41	207.38	1.60	0.07	129,612 $\pm$ 13,312	Caro et al., 2011 [22]
<b>TCR-5</b>	MAD-5762rBIN	Level 9	2–10	2.19	8.23	1.19	11.99	11.99	287.91	2.08	0.08	138,418 $\pm$ 11,673	Caro et al., 2011 [22]

The Marchenilla terrace (+10 m) consists of three sedimentary cycles with decreasing granular size. Pebbles and gravel predominate at the base, while deposits of sand and/or silt are found at the top, forming three alternating layers each about a meter thick. The gravels are lithologically composed of sandstone, limestone, and flint. At the top of the terrace, there is a formation of carbonated soils. The silt layer, which lacks any industries, was dated to approximately  $103,448 \pm 7984$  ka BP using OSL dating (Table 4).

The Torre de la Membrilla terrace is situated at an altitude of +12 m. At the base of its topography, there is a paleobed consisting of an isometric subangular–subrounded gravel conglomerate (5–7 cm in diameter) embedded in a sandy matrix. The lithological composition includes sandstone, limestone, and flint. Within this deposit, the presence of some unrounded (R0) flint flakes of Levallois character was detected (MEM-1).

Lastly, the la Liebre terrace is located at an altitude between +12 and +15 m (LIE-1). In this area, 45 unrounded pieces (R0) of quartzite and 1 small flint flake were recovered from the colluvial deposit. Among the findings, 18 cores stand out, with 11 being centripetal (61%) and averaging between 55 and 60 mm in size, showing several extractions. The remaining cores are simple with few non-hierarchized extractions. Among the 14 simple flake tools, half are semi-cortical, evenly divided between cortical and internal flakes. The recognizable butts are all cortical (nine) or smooth (four), with three instances of suppressed butts. Among the 13 utensils, a stone carved with a unifacial edge, 2 scrapers (simple and double), 3 typical end scrapers, 4 notches, 1 denticulate, and 2 truncated flake tools were found. Retouches are primarily direct, simple, and deep, resulting in sub-parallel end scrapers. Typologically, it is noteworthy that there is an absence of Levallois Group elements, both in the cores and knapping products, indicating the predominance of Group III and notches.

### 3.2. The Upper Pleistocene of Guadalquivir's Terraces

The geomorphological connectivity between the Guadaíra and Guadalquivir rivers occurs at the Guadalquivir's T11 (+44 m) and T12 (+28 m) terraces. From there, a structural hominid dispersion occurred, reaching the top of the Guadalquivir middle terraces, from T11 and T12 to T7 (+95/+100 m). Functional connectivity, on the other hand, occurred throughout the Guadaíra–Guadalquivir floodplain. To describe their geoarchaeology, we followed three criteria: chronostratigraphical, geomorphological, and techno-typological correlations. Using the chronostratigraphical criterion, we took the T11 level in Tarazona as a reference point, which provided a chronology of >129 ka BP (OSL), and the T12 pedological carbonates in Las Jarillas, with a chronology of 80 ka BP (U/Th). Eight lithic assemblages (PIO-1, PIO-2, PIO-3, REY-1, TARIII-1, TARIII-3, TARIII-4, TARIII-5) were selected, forming an Upper Pleistocene chronostratigraphical series. Applying the geomorphological criteria, we included the lake–palustrine sediments and soil horizons at the top of the different terrace levels between T12 (+26–29 m) and T7 (+95–100 m) in the alluvial series of the Upper Pleistocene. Seven lithic assemblages (TARII, TARIII-2, MUH-4, SAL-2, PIO-4, AER-2, REY-3) were identified in these terraces. The lake–palustrine deposits of Saltillo (SAL-3.2) in T10 (+45/+55 m), interpreted as the negative magnetic–stratigraphic Event Biwa 1 (approx. 180,000 BP), were among these findings.

Finally, for the surface sites with geomorphological characteristics, we used the techno-typological characterization criteria to correlate them with assemblages in a stratigraphic position. Eight lithic assemblages (PIL-1, MOL-1, MAJ-1, COR-1, CAL-1, TOR-3, PAD-1, CAS-1) were selected for this purpose.

#### 3.2.1. Gravel Bars of Alluvial Deposits (T11 and T12, Pioneer and Fuente del Rey Sites)

These gravel bars are lithologically composed of quartzite and quartz (75–80%), with the remaining 20–25% consisting of other lithologies, such as sandstone, flint, shale, granite, etc. From Pioneer (PIO-1), a collection of 62 lithic pieces was gathered, with quartzite accounting for 71%, flint for 25%, and other materials for 5%. These pieces were distributed among the cores (32%), flakes (47%), and tools (21%) (Figure 5). Among them, 15% were

bifacial, with the majority exhibiting semi-rounding (R2, 50%) or full rounding (R3, 10%). Noteworthy characteristics include the high percentage of butts in the utensils and the absence of prepared butts. Unelaborated cores were also found, along with a significant abundance of notches and scrapers, which were the only components present. It is worth noting the presence of nodular tooling, dominated by pebbles knapped into handaxes. In Fuente del Rey (REY-1), the tools do not exhibit a specific character. The assemblage consisted of 13 simple flake tools, 13 cores, and 1 duplex utensil, all made of quartzite, except for one flint flake tool. The entire assemblage has been affected by alluvial erosion: 66% strongly (R3), 27% medium (R2), and 7% lightly (R1).

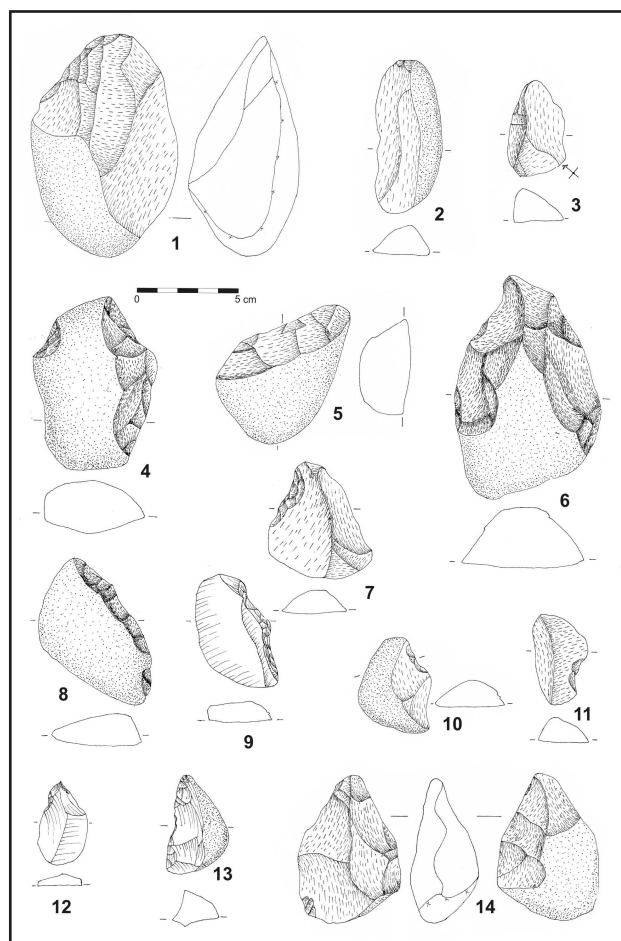


**Figure 5.** Pioneer lithic industry. PIO-1: scrapers (4, 6, and 8), handaxe (14); PIO-2: chopping tool (1), natural backed knives (2), backed knives (3), scraper (5), notch (10); PIO-3: scrapers (7 and 9), notch (11), borers (12 and 13). Raw materials: quartzites (1, 2, 3, 4, 5, 6, 7, 8, 10, 11, and 14); flint (9, 12 and 13).

### 3.2.2. Sand Bars of Alluvial Deposits with Pebble and Fine Gravels in Matrix (T11 Pioneer and Tarazona III Sites)

The lithological composition is dominated by quartzite (60–65%) and quartz (20–25%), accompanied by sandstone, shale, limestone, and other materials. Within the lithic assemblages, simple flakes comprise the majority ( $M = 55\%$ ), followed by cores ( $M = 32\%$ ) and tools ( $M = 17\%$ ). The presence of large tools, specifically trihedrons, is merely sporadic and even less common in PIO-2, where there is only one bifacial index value of 17. Quartzite is the predominant raw material, accounting for over 80% of the assemblages, particularly in the T11 series (TARIII-1, 3, 4, and 5) (Figure 6). However, in the assemblages of T12, the proportion of flint increases (22% in PIO-2 and 50% in PIO-3) (Figure 5).

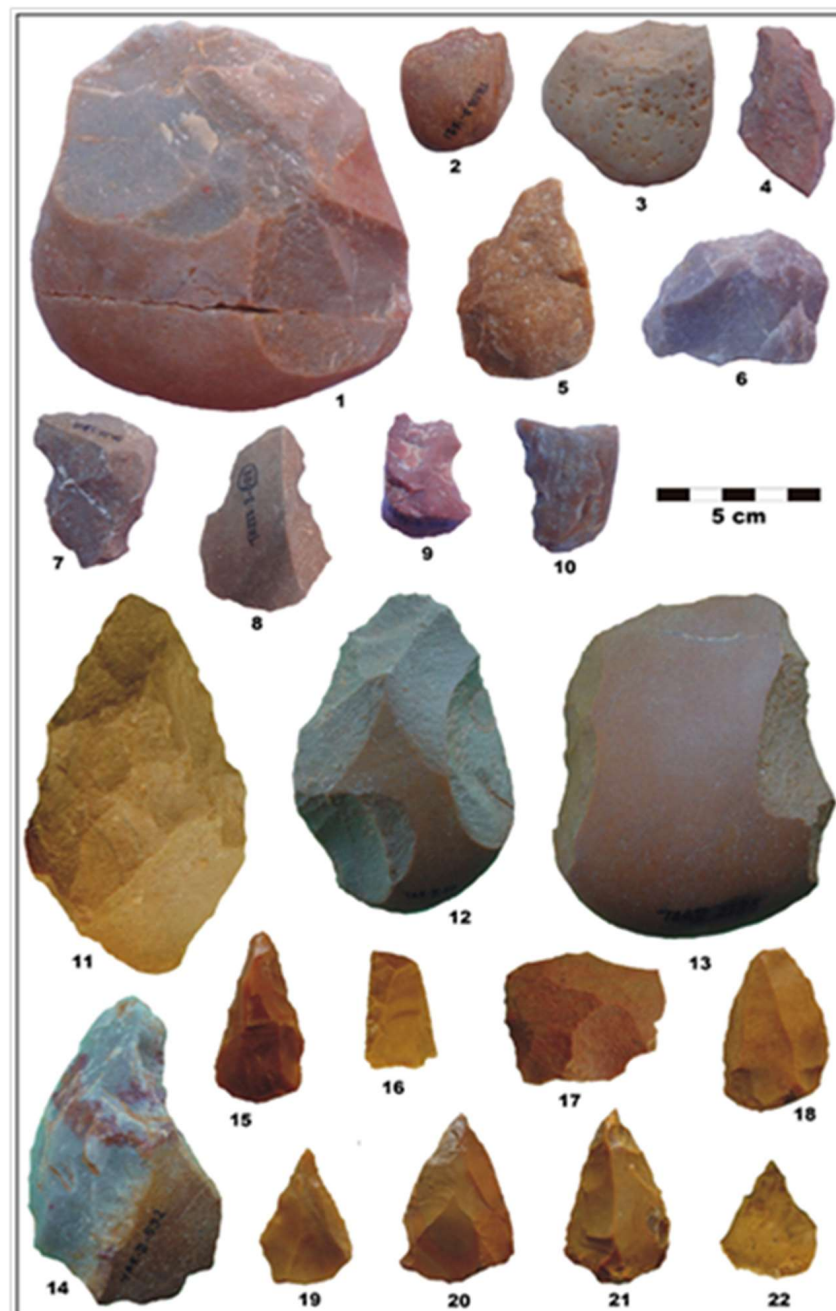


**Figure 6.** Lithic industry. Tarazona III (TARIII-4): choppers (1, 2, and 3); scrapers (4, 5, and 6); notches (7, 8, and 9) and denticulate (10) (in quartzites). Tarazona II (TARII): handaxes (11 and 12); cleaver (13); scrapers (14, 15, and 16); Levallois flake (17); Levallois point (18, 19, and 20); Mousterian point (21) and borer (22). Raw materials: quartzite (11, 12, 13, 14, and 17); flint (15, 16, 18, 19, 20, 21, and 22).

The rounding of the tools exhibits a dual modality: in the T11 series, they appear with little to no rounding (R1 and R0), while in the T12 series, although some elements lack rounding, the majority exhibit a high level of rounding (R2 and R3). From a technological perspective, there is a general absence of the Levallois group, except in PIO-3, where it has a small representation (9%), and there is an acceptable presence of Groups II and III ( $M = 22\%$  and  $20\%$  respectively), except in PIO-2 (3%). Conversely, Group IV is well represented in T11 (15%), while in T12, it appears only minimally, in contrast to the high representation of notches found in every site ( $M = 27\%$ ). The faceting index is minimal or absent throughout the entire series.

### 3.2.3. Massive Loam–Clay or Sandy–Clay Alluvial Deposits (T7 to T12: Muharra, Saltillo, Caleras, Toril, Tarazona II, Tarazona III, Pioneer, Aeropuerto, and Fuente del Rey sites)

The Upper Pleistocene alluvial terraces of the Guadalquivir River frequently exhibit deposits containing pebbles and fine gravels, either suspended within the matrix or found in small channels. The lithology of these pebbles and fine gravels is predominantly composed of quartzite (45%), quartz (25%), quartzite sandstone (15%), and other materials (15%). Quartzite is the primary raw material utilized for knapping in two types of assemblages: those with a minimal presence of flint (MH4, TARIII-2, PIO-4, and REY-3), and those where the flint exceeds 20% (SAL-2, TAR-II, and AER-2). Technologically, simple flakes ( $M = 55\%$ ) and tools ( $>20\%$ ) are prominent. Macro-tools are particularly notable in TAR-II (Figure 6). The artifacts generally appear unrounded (90% R0) or lightly rounded (8% R1), occasionally with some showing moderate rounding (2% R2). The series exhibits significant Levallois indices (Li 16%). In the TARIII-2 series, no Levallois elements are present, perhaps due to the scarcity of recovered artifacts. Group II is the most represented across practically all series, with its peak in AER-2 (78%), consisting primarily of various types of scrapers. Group III is similarly represented ( $M = 15\%$ ) in AER-2 and TARIII-2. Denticulates also appear in similar percentages in the majority of the series ( $M = 5\%$ ), with a notable presence of 14% in TARIII-2. Notches are observed in varying proportions: low ( $M = 8\%$ ), elevated ( $>20\%$ ), and one remarkable case reaching 57% (TARIII-2). The lithic assemblage faceting index in this deposit is one of the highest (Fi 15), although it should be noted that certain assemblages of retouched flakes exhibit considerably higher indices of Fi 25 (SAL-2) or Fi 22 (TARIII-2).

### 3.2.4. Surface Geomorphological Deposits (T6 to T10: Pilar, Molinillos, Majapán, Cortés, Caleras, Toril, Padrecito, and Castilleja sites)

The archaeological sites situated on the surface of geomorphological deposits reveal extensive assemblages characterized by a significant presence of simple flakes ( $M = 47\%$ ), accompanied by a noteworthy abundance of utensils ( $M = 28\%$ ), most of which are in flake form. The Levallois group is well represented in the assemblages ( $M = 14\%$ ), with CAS-1 displaying the highest values (Li 28) (Figure 7), and Group II being the most prominent ( $M = 42\text{--}60\%$ ). Group II consists primarily of various types of scrapers, with simple scrapers being the most common. Group III also exhibits good representation ( $M = 19\%$ ), reaching up to 33% in certain assemblages, making it the most prevalent in CAL-1. Group IV is present in all the assemblages (5–15%), except for TOR-3. Notches are consistently present across all series, typically averaging around 9%. These surface assemblages generally exhibit low faceting indexes, although some pieces show a significant increase in the index value when retouched flakes are included (CAL-1, Fi 29). From a lithological perspective, quartzite dominates the assemblages (92%), while flint comprises a smaller proportion (5–10%). The majority of the series displays unrounded artifacts (90% R0), with elements exhibiting mild rounding (R2) reaching up to 30%. In the higher terraces (T6 and T7), artifacts displaying high levels of rounding (R3) become more prominent.

### 3.3. Raw Material, Lithic Industry Assemblages, and Use–Wear SEM Analyses

This section of the study examines the Middle Paleolithic lithic assemblages found in the open-air archaeological sites situated on the Middle–Low Terraces of the Guadalquivir and Cerro Santisteban, along with five additional archaeological sites that have not yet been published, located in the lower section of the Guadaira slope. In total, the study analyzed and interpreted 28 archaeological sites.

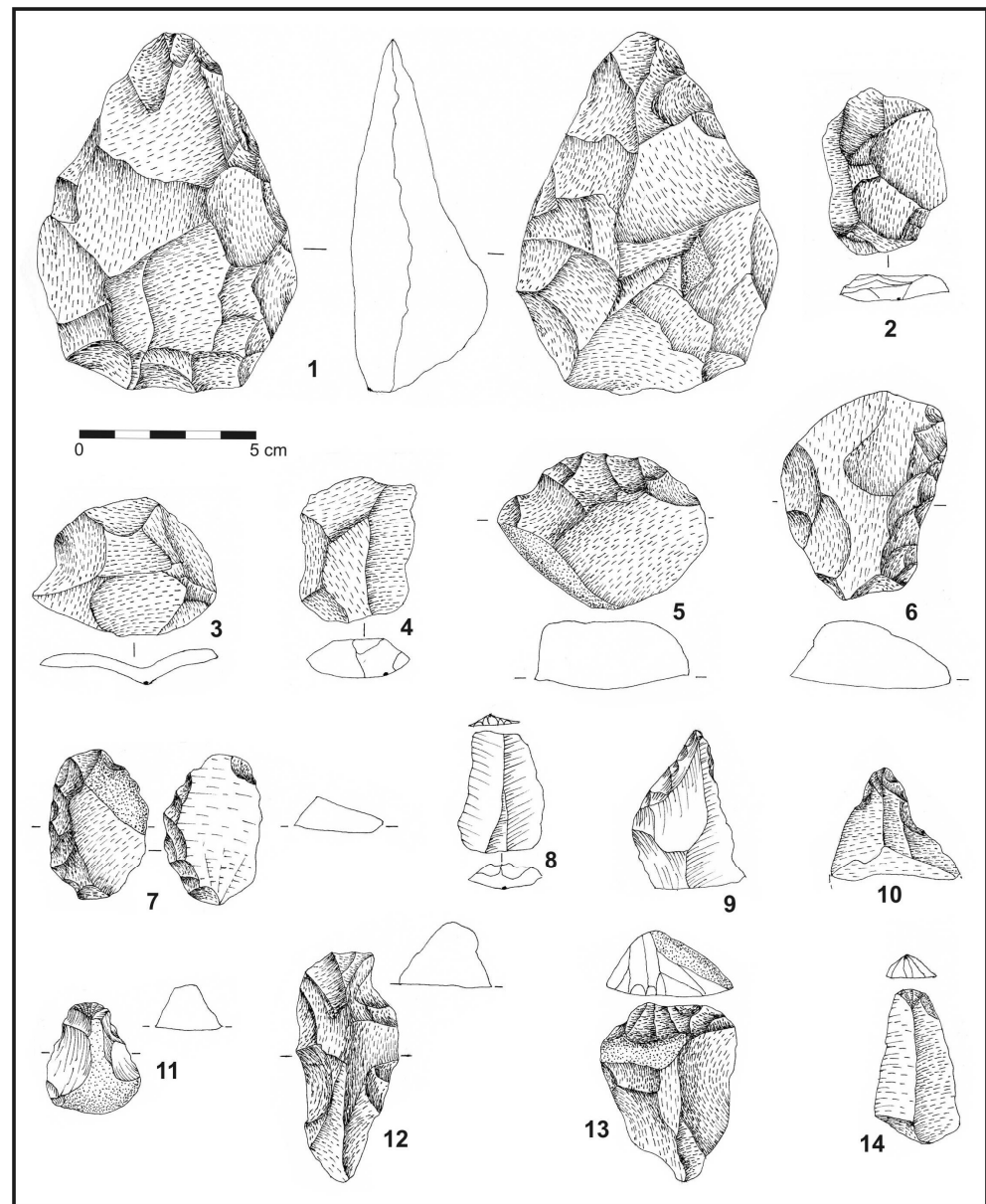


**Figure 7.** Castilleja (CAS-1) lithic industry: Handaxe (1), Levallois flakes (2, 3, and 4), scrapers (5, 6, and 7), truncated piece (8), borers (9 and 10), end scrapers (11, 12, 13, and 14). Raw materials: quartzite (1, 2, 3, 4, 5, 6, 7, 10, 12, and 13); flint (8, 9, and 11).

### 3.3.1. Raw Material: Significant Geographical Distribution of Archaeological Sites

The search for higher-quality raw materials for knapping was a consistent pursuit during the Middle Paleolithic [55–59]. In line with this interpretation, recent studies have emphasized the role of medium-sized tributary rivers' watersheds as a geoarchaeological framework for developing mobility strategies, including the search for raw materials and the implementation of subsistence activities [8,60,61]. Thus, in this regard, we offer an interpretation of the connectivity between the Guadalquivir and Guadaíra watersheds. The presence of Middle Paleolithic lithic industries, consisting of well-crafted flint and quartzite knapped in situ, serves as the geoarchaeological evidence for hominid mobility strategies during the late Middle Pleistocene (TAR-II) and the entire Upper Pleistocene period (Figure 8).

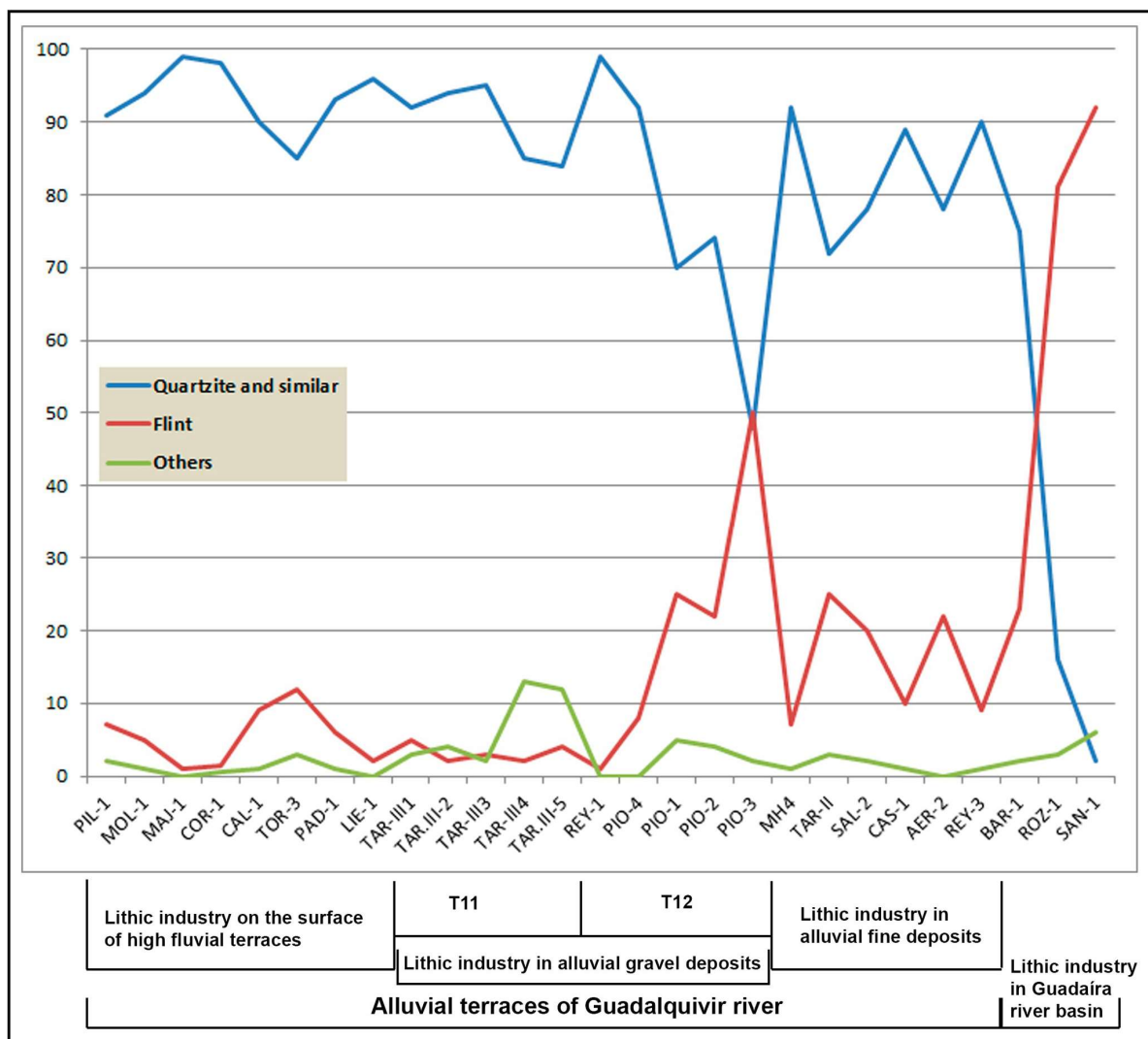


**Figure 8.** Comparative graph of the use of raw materials in percentages in the different geomorphological areas of the HAC.

The lithic assemblages obtained exhibit minimal or no displacement (R0). This mobility strategy is evident in two significant geographical references: first, the distribution of quartzite pebbles from the Guadalquivir’s alluvial deposits, which were transported by hominids to the Guadaíra watershed for in situ knapping; second, the presence of flint lithic assemblages that were transported from the Subbetic limestone outcrops in the Guadaíra region to the archaeological sites in the Guadalquivir alluvial terraces, where they were also knapped in situ.

In the deposits of the Guadalquivir’s T10, T11, and T12 Middle Terraces, which consist of channel bars and lake–palustrine sediments, the Middle Paleolithic assemblages are predominantly made of quartzite raw material ( $M = 70–80\%$ ). The presence of flint ranges from 25% to 50% in the T12 deposits, which can be attributed to the Subbetic outcrops located approximately 44 km away in a straight line or slightly more (50 km) following the Guadaíra–Rozalejo thalweg. The lithic industries found at the top of these alluvial terraces are associated with hydromorphic formations (10YR) or Vertisol soils (TARIII-2, 10 YR 6/4), all of which are younger than 104 ka BP [22,23]. The lithic artifacts found in these deposits are mostly unrounded (R0) and made of quartzite (85%).

In the Guadaíra region, where it intersects with the limestones and flint of the Subbetic units, the Middle Paleolithic industries are consistently characterized by unrounded artifacts (R0) (SAN-1). The two highest-quality raw materials used for lithic knapping in this area are flint and quartzite. Since there are no Paleozoic quartzite outcrops within the Guadaíra watershed, the quartzite pebbles used in knapping are believed to have come from the alluvial deposits of the Guadalquivir terraces. The Rozalejo River archaeological site served as a gathering spot for hominids to obtain quartzite raw material. Therefore, the absence of rounded artifacts (R0) suggests that the quartzite was knapped in situ.

The Santisteban archaeological site (SAN) presents a different scenario. It is located in the piedmont of the Sierra de Esparteros, and its lithic industry consists entirely of flint. The assemblages at this site date from the Middle Pleistocene to the beginning of the Upper Pleistocene.

### 3.3.2. Lithic Industry Assemblages and Techno-Typological Analysis

The lithic assemblages in these sites are characterized by the dominance of cores and flakes, occasionally accompanied by macro-tools. Discoidal cores of various sizes, ranging from middle-sized (5–7 cm) to small cores (2–4 cm), derived from knapping waste, are common in these assemblages. The presence of flint in a site is often associated with a more diverse range of flake tools, including scrapers, notches, and end scrapers. There seems to be a relationship between the increased use of flint and the development of more complex technical processes. A faceting index (Fi) value of  $\geq 10$  is typically observed in lithic assemblages with a significant percentage of flint ( $\geq 20$ ). These assemblages are found in loam–clay or sandy–clay deposits at the top of alluvial terraces, either on the geomorphological surface of the terrace or in detritic fills in the karstic piedmont. However, it should be noted that a high percentage of flint does not always correlate with a high faceting index (Fi), as it may be the case when smaller lithic assemblages or incomplete operational chains are found. The lithic industries in the mentioned loam–clay or sandy–clay deposits exhibit a higher Levallois index (Li). Similarly, lithic assemblages on the geomorphological surface, composed of flint and quartzite, show a high faceting index (Fi) on the butts of the tools. In terms of the progressive increase in the use of flint in different archaeological sites, it does not correspond to a regression curve, which indicates a minimal increase in the application of the Levallois technique (Figure 9). Furthermore, the Levallois transformation index (Lti) is generally very high in almost all lithic assemblages where this technique is present, regardless of the quantity of raw material used.

The techno-typological analysis revealed that Group II (Middle Paleolithic) predominates throughout the archaeological sequence, although other technical groups coexist. Group I (Levallois) stands out in three geoarchaeological formations: karstic fill, loam–clay or sandy–clay alluvial deposits, and superficial deposits. Denticulates (Group IV) and notches are most commonly found in assemblages associated with gravel and sandy deposits, as well as some on the geomorphological surface. Group III (Upper Paleolithic), although less numerous, is well represented in some archaeological series on the surface and in loam–clay or sandy–clay deposits. From a chronostratigraphic perspective, there is an observed increase in Group II and, especially, Group I from the oldest to the most recent series. Conversely, denticulates and notches, which have prominent percentages in the oldest series, decrease in importance in more recent assemblages.

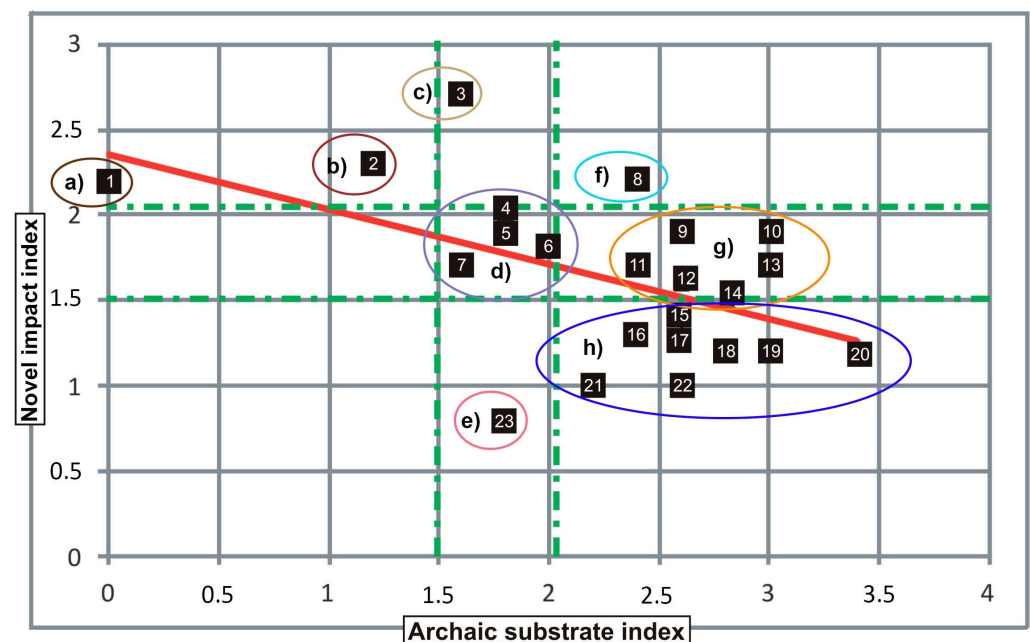


**Figure 9.** Relationship between the indices of the characterizing traits of the two groups of Middle Paleolithic lithic assemblages present in the Guadaira–Guadalquivir human corridor: archaic substratum index (ISA) and novel impact index (IIN). The combination of both indices defines the following groupings: (a) No substratum and high impact: SAN-1 (1); (b) low substratum and high impact: BAR-1 (2); (c) medium substratum and high impact: TARII-1 (3); (d) medium substratum and medium impact: CAL-1 (7), PIO-3 (5), SAL-2 (4), and TOR-3 (6); (e) medium substratum and low impact: TARIII-2 (23); (f) high substratum and high impact: CAS-1 (8); (g) high substratum and medium impact: REY-3 (11); MOL-1 (12); PIO-4 (9); PAD-1 (13); PIL-1 (10), and MAJ-1 (14); (h) high substratum and low impact: TARIII-1 (20), 3 (17), 4 (15); PIO-2 (19); MH4 (18); COR-1 (22); PIO-1 (16) and AER-2 (21). The trend line is displayed in red color.

These assemblages exhibit sequential continuity and can be divided into two major periods. The first period corresponds to the Acheulian tradition (archaic substrate) [17,62], found in the gravel bars of alluvial deposits, loam–clay and sandy–clay deposits at the top, and the most recent alluvial terraces of the Guadalquivir [14,16–20,22,23]. Characteristics of this period include the knapping of rounded pebbles, a high percentage of quartzite, limited flake varieties, and repetition of Early Paleolithic types. The second period corresponds to the progressive introduction of the Levallois technique, identified in archaeological sites located in sandy–loam and hydromorphic soils at the top of the Guadaira alluvial terraces. This period is characterized by a higher number of artifacts, the generalization of the Levallois knapping technique, an abundance of centripetal cores, improved retouching, an enrichment of Group II, an increase in Group III, and the use of flint as a raw material (Figures 9 and 10). It should be noted that the lithic assemblages from the Santisteban karstic fill show no evidence of the Acheulian technological tradition and represent a classic Middle Paleolithic assemblage [62].

### 3.3.3. Use–Wear on the Quartzite Pieces’ Edges: SEM Analysis

Scanning electron microscopy (SEM) analysis was conducted on six unrounded quartzite pieces (R0) from the archaeological site of Tarazona III. Five of these pieces were recovered from level TARIII-4, consisting of one borer (B), two denticulates (D1 and D2), one multiple piece (MP), and one double notch (DN). One atypical borer (AB) was found in level TARIII-5, which is characterized by *floating gravel* facies (matrix-supported gravels). All these pieces were made from fine-grained microcrystalline quartzite without any microfractures in the petrologic microstructure.

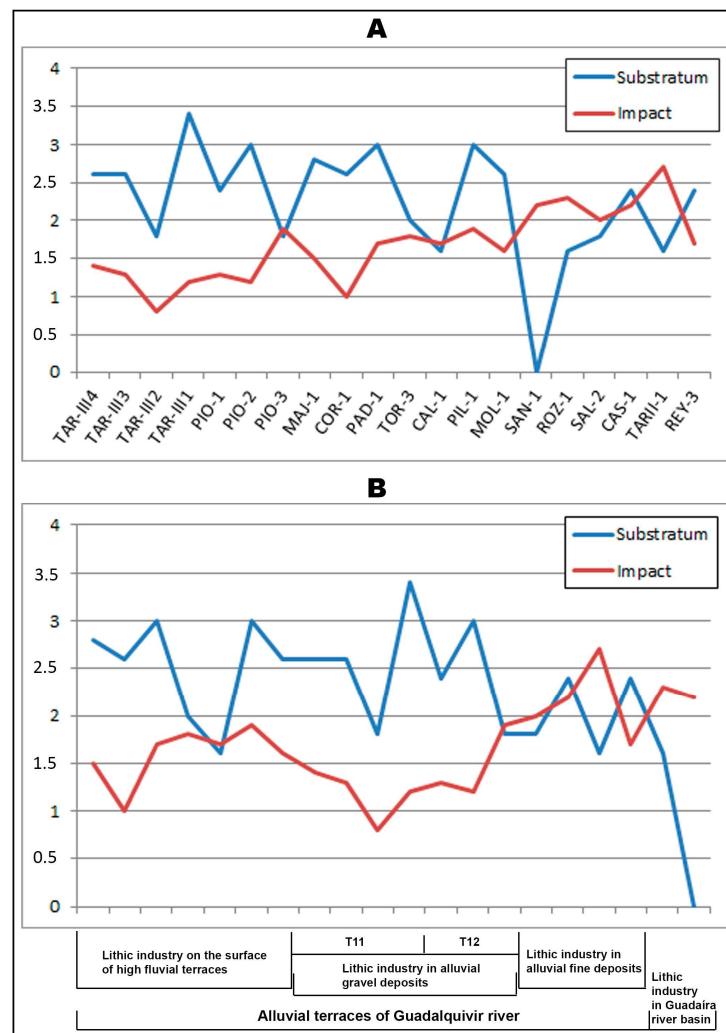


**Figure 10.** Comparative graphs of the characterizing techno-typological features of the two middle Paleolithic lithic assemblages present in the Guadaíra–Guadalquivir hominid corridor: those that maintained the Acheulean tradition (archaic substratum) and those that incorporated the new cultural guidelines (novel impact). (A) Sorted in chronological order; (B) sorted by geomorphological areas.

In addition, an experiment was conducted where several retouched pieces were carved, including notches and denticulates. Among the pieces obtained, a fine-grained internal quartzite flake with a smooth top and a Siret-type fracture, denticulated, was selected and is referred to as M2 Exp.

1. Use–Wear on TARIII-4-level pieces

The microwear analysis of the borer (B) revealed a generalized micro-polishing distribution along the edges. Different sections can be distinguished: the external section shows polished ridges and valleys (Figure 11(1)), while the inner section of the blade exhibits micro-polishing on the ridges with minimal wear on the valleys. It is relevant to note that we use the terms ridges and valleys, while Gibaja et al. [45] refer to *raised* and *recessed* zones. Upon closer examination, the micro-polishing disappears, but a light compaction of the granular surface can be observed in both the elevated zones and recesses.

The denticulates (D1, D2) show different features. Denticulate (D1), with a circular shape, has a well-developed notch with a thick edge and a microdenticulated outline of 6.78 mm with several rabbets around 1 mm (Figure 11(2)).

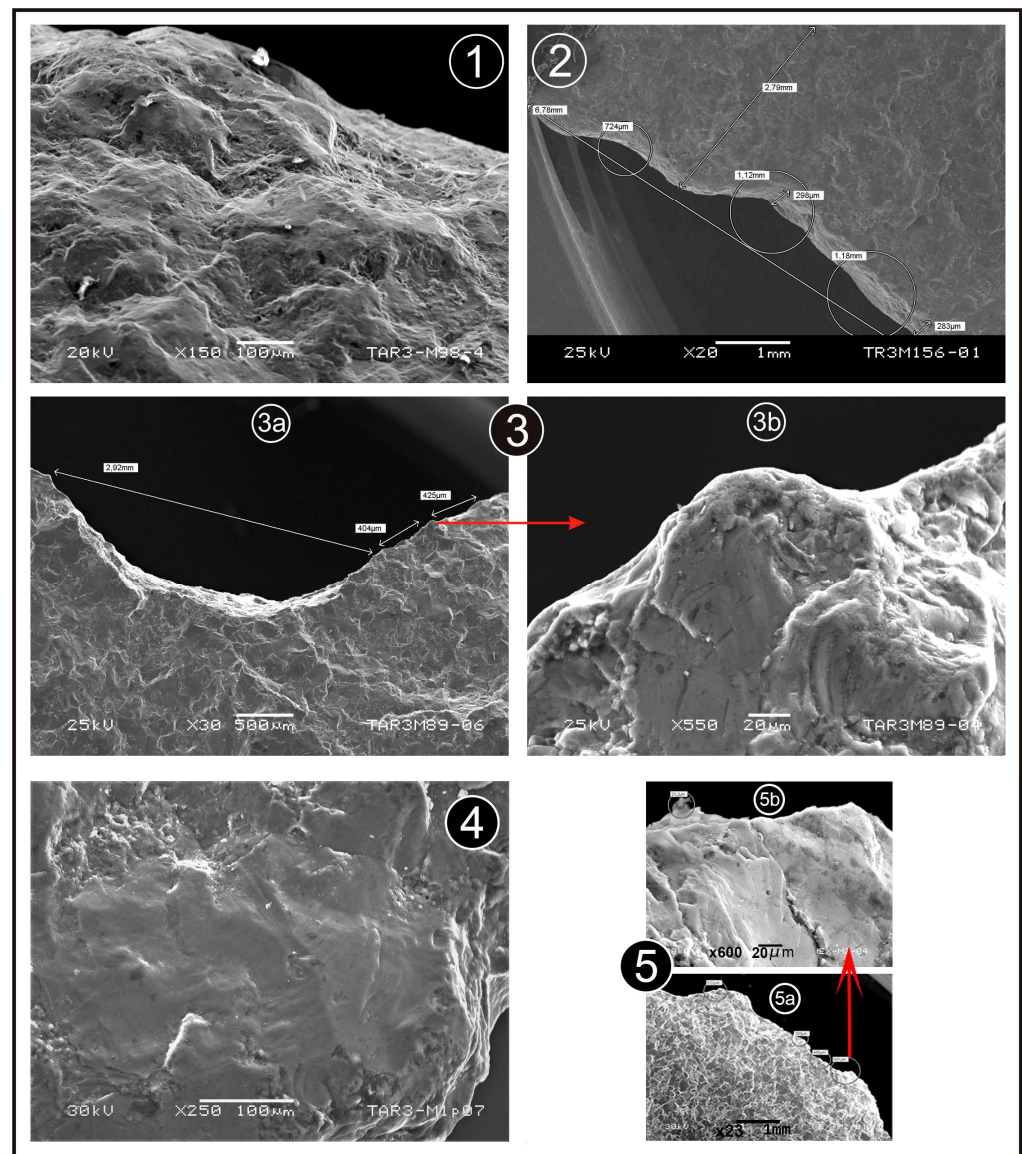


**Figure 11.** Traces of wear on quartzite flakes: (1) Borer (B) of TARI-4. Surface close to the edge, with an intense micro-polishing, both on edges and valleys. (2) Denticulate (D1) of TARI-4. Edge with microdenticulate delineation, with traces of use that diminish in intensity towards the interior of the piece. (3) Denticulate (D2) of TARI-4. (3a) Small-scale view ( $\times 30$ ) of one of the concavities in which the deepest area hardly shows any signs of use, while in the outermost area, the polishing is intense; (3b) detail ( $\times 550$ ) of an external area where the intensity of the traces of use can be appreciated. (4) Atypical borer (AB) of TARI-5. Intense micro-polishing in the areas closest to the edge, both in valleys and on edges. (5) Experimental piece carved (M2.Exp.). (5a) The edge used shows a general microdenticulation on a small scale ( $\times 23$ ); (5b) on a large scale ( $\times 600$ ), micro-polishes and grooves that reach 1 mm towards the interior of the piece can be observed.

The analysis of the edges showed ridges with more use-wear than in the valleys. On the blade, we distinguished three possible affected sections by the use-wear, with different sizes from the external zone to the D1 centers: (1) The first section has a size of around 50 microns, presenting polishing on the ridges but not *recessed zones* (valleys). (2) The second section measures 170 microns approximately, and it has partially lost the polishing of the use-wear. In these ridges, intense wear of the valley zones is recognized, with perpendicular scratches micrometers in size. (3) The farthest section from the denticulate edge ( $>225$  microns) does not show any use-wear sign on the thick ridge or on the

microdenticulated edge design. Denticulate D2, near their edge, has expanding waves, which are the remains of knapping affected by light marks of use–wear on the ridges, and a superimposed posterior impact that sharpened some of the ridges (Figure 11(3a)). On this same edge, we can distinguish a wide notch (2.9 mm) in the deepest area where there are no traces of wear, only a clear line of fragility produced by the carving (Figure 11(3a)). However, on both sides of the notch, we can distinguish small microdenticulated protrusions (around 400 microns), which present a high degree of wear and micro-polishing (Figure 11(3b)), evidencing some use of this area of the piece. The multiple piece (MP) consists of a transverse concave scraper, with two contiguous lateral notches forming a large denticulate. The second piece analyzed is one double notch (DN). Neither of them shows signs of use–wear or micro-polishing nor any other modification on their structure, with all their edges sharp without polishing.

The microwear analysis indicated that the polishing observed on the ridges and valleys of the TARIII-4 pieces suggests effective use–wear, except for the unused MP piece. The concentrated use–wear is mainly found along the edge and extends inward up to 200 microns. The borer and denticulates exhibit moderate uni-directional use–wear, indicating their functional usage. The D1 denticulate shows signs of use but to a lesser extent, as the polishing does not extend beyond its edge microscopically. On the other hand, the notch of denticulate D2 demonstrates a greater degree of use. However, it is possible that the notch could be the result of the later reuse of the piece, either through intentional knapping or as a result of a fracture caused by the knapping process. It is not possible to determine the exact cause of the notch.

## 2. Use–Wear on TARIII-5 level pieces

The SEM analysis of the atypical borer (AB) revealed interesting findings. At low magnification (x65), it is observed that the concavities resulting from knapping are directed towards the interior of the piece, with occasional small, superimposed concavities. The interior of the notched ridge shows nearby areas with polishing, which also affects the waves of the knapping. At higher magnification (x500), the ridges exhibit a higher degree of polish, and perpendicular scratches are observed dropping towards the *recessed zones* [45], which also present some polishing (Figure 11(4)). However, the ridges and valleys in areas such as the end of the notch and the left edge of the piece do not exhibit use–wear.

The atypical borer (AB) shows signs of use primarily in the area around the notched edge. The presence of superimposed concavities in this area suggests that they could have been caused by previous mechanical impacts within the deposit or during use. It is worth noting that the use of the piece seems to be more related to the notch rather than the perforator tip or the adjacent edges.

## 3. Use–Wear on M2 Experimental carved piece

The M2 Exp. denticulate exhibits significant similarities to the denticulates found in archaeological sites. In the experiment, the M2 Exp. piece was used to saw olive wood for a duration of 15 min. A comparison between the experimental edge and the archaeological pieces from the deposits revealed that the former appeared generally more irregular and serrated in nature. As a result of the wood-sawing activity, the edge of the M2 Exp. denticulate displayed evident signs of use–wear extending inward for approximately 700 microns. This use–wear affected the entire undulations of the knapping on the edge (Figure 11(5a)). Notably, a microdenticulated ridge measuring less than 0.5 mm was identified, exhibiting pronounced polishing and featuring distinctive use–wear characteristics. These characteristics included small worn-down areas, micro-polishing on the sharp ridges with a tendency towards rounding, and distinct stripes running in various directions, all of which are indicative of the piece's use in wood-related tasks. Moreover, the concavities of the microdenticulated ridge, located towards the end of the edge, were found to contain remnants of olive wood adhered to them (Figure 11(5b)).

Comparing the details of the M2 Exp. experimental piece with the archaeological TARIII-4 D1 and D2 denticulates, which are unrounded quartzite pieces (R0), we found

some similarities in the distribution of the knapping and use-related ridges. However, the M2 Exp. piece exhibits less polishing and less disaggregation of quartz microcrystals. On the other hand, the archaeological pieces show a deeper and more pronounced wear, without any microcrystal disaggregation. This characteristic can be attributed to three possible causes: the reutilization of the pieces, their use on materials other than olive wood, or their multifunctional nature.

#### 4. Use–Wear general functional interpretation

The microwear traits observed on the edges of the analyzed pieces (borer and denticulates) do not provide definitive evidence of their specific functions. However, the presence of surface polishing, predominantly perpendicular and unidirectional, suggests that these pieces were likely used in a transverse manner along the edge. They could have been employed for activities such as cutting, cleaning, or sharpening the woody stems of trees or scrub branches. In the absence of palynological registers for this area, which may imply paleo-environmental changes in the vegetation coverage (passing from thermo-Mediterranean conditions (olive groves) to a meso-Mediterranean climate (oaks)), and since there are no pedo-sedimentological climate archives, we discarded changes in the vegetal species.

To confirm these potential uses, we compared the wear patterns of these pieces with the use–wear observed on the M2 Exp. experimental piece. The reutilization of lithic pieces, which involves either reuse in such a way that the destined use of the pieces is changed (recycling) or recovery of the piece (retrieval) [63], was not identified in the lithic assemblages of the hominid alluvial corridor of the Guadaíra and Guadalquivir Rivers. Consequently, what remains consistent throughout the archaeological sites within the HAC are the frequent and recurring visits by the same hominid group, characterized by a consistent techno-typological tradition and functional strategies. These practices were passed down from one generation to the next, spanning from MIS6/MIS5 to MIS3.

When comparing our results with the findings of the use–wear analyses, it became apparent how challenging it is to identify the specific functions of Middle Paleolithic pieces. However, certain sites have provided evidence of recycling and retrieval practices. For example, in the Arlanza Valley (Burgos), Middle Paleolithic lithic assemblages showed intensive exploitation of flint and quartzite, indicating a recycling approach [64]. Similarly, the lithic workshop in El Cañaveral (Madrid) utilized old industries in flint sourced from the Acheulian and Mousterian colluvial deposits, demonstrating a retrieval strategy [65]. The El Esquilleu rock shelter in Picos de Europa (Santander) also exhibited recycling processes associated with changes in the operational chain during MIS3 [66,67].

In the Therdonne and Biache–Saint–Vaast archaeological sites from MIS7–6, Levallois points were identified as potential butchery knives, characterized by triangular flakes without a clear form–function relationship [62]. Microwear analyses of chipped edges on some denticulates suggested their use in penetrating animal carcasses, a hypothesis supported by experimental knapping [62]. Moreover, microwear analyses of small flakes in flint from Qesem Cave (Israel), dating back to the Middle Pleistocene Acheulo–Yabrudian Cultural Complex, revealed their use in longitudinal cutting movements associated with butchery activities [68]. This functional interpretation was confirmed through residue detection using Fourier transform infrared spectroscopy and experimental analysis on organic remains [62].

Functional analyses of Middle Paleolithic bifaces from Terra Amata (MIS11–MIS10) and Lazaret Cave (MIS6) in Nice (France) indicated their use in linear longitudinal movements [69]. At the same site, the functional analysis of Quina and demi–Quina scrapers, made of flint, demonstrated their predominantly transverse use in scraping activities related to hide processing. The scraping actions left longitudinal signs, both unidirectional and bidirectional, associated with cutting [70]. Lastly, lithic pieces from the Benzú rock shelter archaeological site exhibited deep and direct use–wear, indicating their use in cutting hides [71].

#### 4. Discussion: Technological Strategies and Functionality in Guadaíra–Guadalquivir’s HAC

Geomorphological structural connectivity has been a commonly applied concept in the study of Paleolithic watersheds. The Somme Valley, in particular, has served as a model for understanding hominid dispersion during the Middle Paleolithic [72,73]. On a larger scale, the Central Asian piedmont of Tien Shan in southeastern Kazakhstan has been proposed as a refuge for hominids during extreme climatic phases. Fitzsimmons et al. [12] recently interpreted the dispersion of archaeological sites as evidence of the piedmont’s significance as a geomorphological unit facilitating structural connectivity between Southern and Northern–Central Asia, contributing to the increased occupation of open-air sites after 40,000 years before present (BP).

At a more localized level, there are cases such as the archaeological sites of Les Fieux in Quercy, France, where the connection between geomorphological units facilitated hominid dispersal over distances of at least 30 km in search of flint outcrops for lithic knapping [11]. Handaxes are found in places farther away from the production areas, occasionally accompanied by Levallois flakes, retouched tools, and cores. In the Garonne watershed in France, structural connectivity was established through geomorphological units similar to those of the Guadaíra and Guadalquivir Rivers: karst, piedmont, and alluvial terraces. There, during the Upper Paleolithic (MIS3 and MIS2), evidence of a bi-directional corridor towards the Atlantic and the Mediterranean was observed, indicating significant human movement [9].

The availability of high-quality raw materials, such as flint, cherts, quartz, quartzites, limestones, and iron nodules, has also been emphasized in the environment of the El Esquilleu cave in Picos de Europa, Santander, Spain. The abundance of quality raw materials in El Esquilleu favored lithic recycling as opposed to other strategies. Similar situations can be seen in the open-air archaeological sites in the alluvial terraces of the Miño River Valley in Galicia, Spain [7,13], and in the local model of a corridor proposed by Browne et Wilson [4], with its center at the Bau de l’Aubesir archaeological site, which exhibits a wide diversity of raw materials (46 types) and 110 source areas in Mont Vaucluse, France.

In many European geographic areas, the Middle Paleolithic period advancements and expansions in technological innovations, accompanied by cultural changes and specialized food-gathering practices, led to modifications in the patterns of territorial dispersion [8–11,55,56,64,65]. These mechanisms resulted in different types of occupations (stational or specialized), resulting in a diversity of archaeological sites. We determined whether they were stational or specialized based on the functionality of the lithic tool-kit found in the assemblages.

Access to the primary geological outcrops, serving as supply areas for raw materials, was a recurring practice in the alluvial plains of major rivers. This was facilitated by the tributaries, with routes spanning less than 50 km, creating alluvial corridors where hominids established themselves. The excellent geomorphological structural connectivity, connecting floodplains, alluvial terraces, and piedmonts, favored the formation of these corridors.

Within the Paleolithic sequence of the Guadalquivir River, the main open-air archaeological site of the Middle Paleolithic is Tarazona (TARIII, MIS6–MIS5, Late Middle Paleolithic). The site exhibits techno-complexes consisting of 2479 quartzite pieces, primarily small flakes, with fewer cores, and a low presence of macro-tools [22,23]. Another significant archaeological site is the karstic fill of the Cerro Santisteban (1,656 pieces) in the Sierra de Espartero piedmont, which represents a classic Middle Paleolithic sequence of flint [46]. This paper provides a chronology of the Middle–Upper Pleistocene (136–74 ka BPU/Th) based on bones found in the karstic fill. The Guadaíra and Guadalquivir Rivers’ geomorphological connectivity occurs between these two sites, with a distance of 44 km in a straight line or slightly more (50 km) following the Guadaíra–Rozalejo’s thalweg (Figure 12). From a chronostratigraphic perspective, the Middle Paleolithic period in the Guadaíra–Guadalquivir region can be divided into two chronological blocks:

- (1) The first block, of relatively short duration, occurred from the end of the Middle Pleistocene to the beginning of the Upper Pleistocene (MIS6/MIS5) (>129 ka BP and

- <104 ka BP). During this period, there was a prevalence of notches, scrapers, and knapped pebbles in quartzite, indicating a high persistence of the archaic substratum and limited relevance of newer tendencies (TARIII-4 and 5, PION-1, 2, and 3).
- (2) The second block, of much longer duration, took place during the Upper Pleistocene (MIS3) (<110 ka BP and possibly even 50 ka BP). This block is characterized by lithic assemblages that exhibit a wide diversity of flake tools, including the presence of the Levallois technique and signs of bifacial tools. The influence of new techno-typological methods has become more evident, although the archaic Acheulian substratum continued to persist (TARII, TARIII-1, 2, and 3, SAL-2, CAS-1, MH4, PIO-4, AER-2, REY-1 and 3, PIL-1, MOL-1, MAJ-1, COR-1, CAL-1, TOR-3, PAD-1, BAR-1, MEM-1, LIE-1, ROZ-1, and SAN-1). Among these archaeological sites, only Santisteban and Membrilla feature industries exclusively in flint. In sites like ROZ-1, TARII, AER-2, PIO-1, 2, 3, BAR-1, and SAL-2, their assemblages have a high percentage of flint (>20%), while the rest of the archaeological sites primarily contain quartzites.

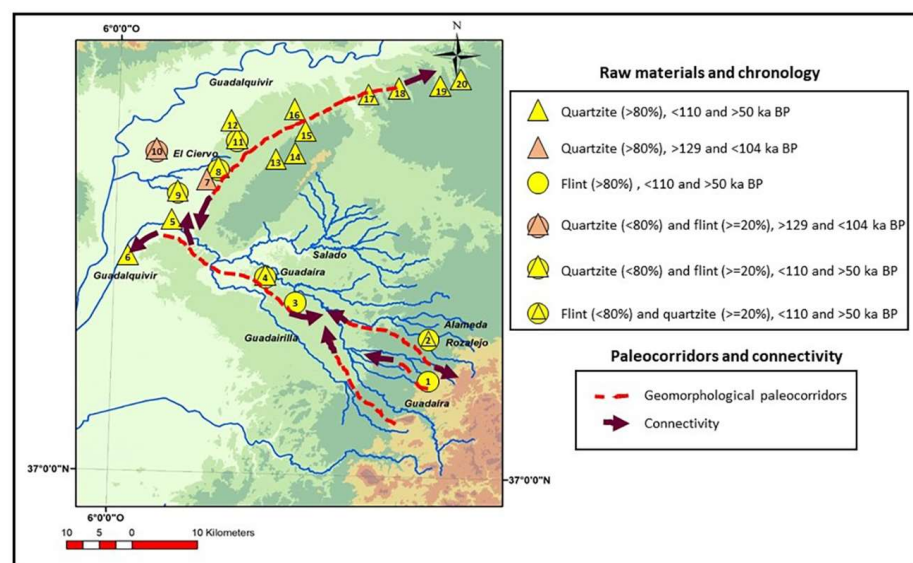


**Figure 12.** Hominid dispersion model between the Guadalquivir terraces and Betic mountains, indicating geomorphological paleocorridors and the connectivity between them, and the location of the deposits grouped according to the predominance of the raw material (quartzite and flint), as well as their chronology ascription: (1) >129 ka BP and <104 ka BP; (2) <110 ka BP, and even of 50 ka BP.

According to the functionality criteria applied in the interpretation of the lithic assemblages at archaeological sites, four types of settlements were identified, which are associated with the dispersal of hominid hunter–gatherer groups (Table 5): (1) Habitual or Recurrent Sites (HS) (TARIII-4, TARII, CAS-1, SAL-2, SAN-1, PAD-1, PIL-1)—these sites exhibit the following features: complete or nearly complete operative chains, a high percentage of tools (>30%), and a significant proportion of non-rounded industries (R0 or R1). (2) Temporary Sites (TS) (MAJ-1, TARIII-2, TOR-3, AR-2, PIO-4, PIO-4, REY-3, LIE-1, BAR-1, COR-1, CAL-1, ROZ-1)—this category is characterized by incomplete operative chains, but with enough pieces to reconstruct the operative chain. There is a low proportion of tools (<30%), but a high occurrence of repeated items (possible specialized sites). Non-rounded industries (R0 or R1) dominate in these sites. (3) Lithic Workshops (LW) (MUH-1, TARIII-3, MOL-1, TARIII-1)—these are distinguished by an abundance of knapped flakes and cores (derived from geological outcrops in situ or ex situ, and transported to the archaeological site), along with a low representation of tools. (4) Indeterminate (IN) (TARIII-5, PIO-1, PIO-2, PIO-3, REY-1, REY-2)—the lithic pieces found at these archaeological sites do not exhibit well-defined characteristics, leading us to categorize them as indeterminate. None of these sites are associated with butchering or hunting activities.

**Table 5.** Proposal on the functionality of the HAC deposits. Functionality site: habitual site (HS) ; temporary site (TS) ; lithic workshop (LW) ; indeterminate (IN) . Rounded industry: unrounded (R0); less rounded (R1); middle rounded (R2); very rounded (R3). Technical balance: the closer to 1, the more balanced results of the series; the closer to 0, the fewer flakes in the series; higher than 1 indicates fewer cores in the series. Technical balance index of the series responds to the LN/EX relationship, where LN is the result of dividing the total number of carving products by the total number of core supports and EX, which is the visible number of extractions of core supports; the closer the index is to 1, the more balanced the set is; the closer to 0, the fewer the flakes in the set, while values greater than 1 denote core-poor series.

Archaeological Site	Terrace Level	Deposit	Pieces n°	Retouched Tools (%)	Technical Balance	Raw Material (%)			Rounded Industry (%)				Functionality Site			
						QUARTZITE	Flint	Other	R0	R1	R2	≥R3	HS	TS	LW	IN
TARIII-4	T11	Gravel bars	1275	31	0.34	85	2	13	60	30	9	1	yes			
TAR-II	T11	Loam-clay	2885	30	0.47	72	25	3	95	5	0	0	yes			
CAS-1	T10	Geomorph. surface	330	30	0.96	89	10	1	85	14	1	0	yes			
SAL-2	T10	Loam-clay	312	33	1	78	20	2	81	17	2	0	yes			
SAN-1		Karst detrial fill	1656	36	5.5	2	92	6	100	0	0	0	yes			
MAJ-1	T6	Geomorph. surface	195	33	0.22	1	0		0	58	37	5	yes?	yes?		
TARIII-2	T11	Loam-clay	118	31	0.67	94	2	4	95	5	0	0		yes		
TOR-3	T7	Geomorph. surface	190	31	0.67	12	3		94	6	0	0		yes		
PIO-4	T12	Loam-clay	54	48	1	92	8	0	90	4	6	0		yes?		
REY-3	T12	Loam-clay	128	24	1	90	9	1	58	40	2	0		yes?		
LIE-1		Geomorph. surface	45	29	0.2	96	2	0	100	0	0	0		yes?		
BAR-1		Geomorph. surface	44	38	0.47	75	23	2	75	25	0	0		yes?		
COR-1	T6	Geomorph. surface	222	25	0.25	1,5	0.5		0	54	44	2		yes?		
CAL-1	T8	Geomorph. surface	91	31	0.42	9	1		20	79	1	0		yes?		
AER-2	T12	Loam-clay	45	22	1.13	78	22	0	16	84	0	0		yes?	yes?	
PAD-1	T7	Geomorph. surface	950	22	0.5	6	1		14	51	28	7		yes?	yes?	
PIL-1	T9	Geomorph. surface	590	19	0.75	7	2		91	8	1	0		yes?	yes?	
ROZ-1		Geomorph. surface	228	16	0,7	15	83	2	68	26	5	1		yes?	yes?	
MUH-4	T7	Loam-clay	273	18	1	92	7	1	96	4	0	0		yes?	yes	
TARIII-3	T11	Gravel and sand bars	727	17	0.5	95	3	2	95	5	0	0			yes	
MOL-1	T9	Geomorph. surface	2159	14	0.38	5	1		4	92	4	0			yes	
TARIII-1	T11	Gravel bars	264	20	0.67	92	5	3	99	1	0	0			yes?	
TARIII-5	T11	Gravels bars	25	16	0,2	84	4	12	95	5	0	0				yes
PIO-1	T12	Gravels and sand bars	62	21	0.33	70	25	5	11	27	51	11				yes
PIO-2	T12	Gravels and sand bars	222	17	0.35	74	22	4	7	37	38	18				yes
PIO-3	T12	Gravels bars	108	19	1.53	48	50	2	17	43	31	9				yes
REY-1	T12	Gravels and sand bars	27	4	0.2	99	1	0	0	7	27	64				yes
MEM-1	T (+12m)	Gravels and fine gravels	3	0	-	0	3	0	3	0	0	0				yes

Consequently, the HAC corridor in the Guadaíra–Guadalquivir region serves as a multifunctional corridor, with three primary types of activities: the provisioning and distribution of raw materials, lithic knapping, and anthropic activities, indicating the use of industry. The analysis of use–wear patterns, as well as the comparison with the experimental piece M2 Exp, indicates that the lithic pieces were not repetitively used. This finding reinforces the notion that the corridor facilitated the immediate provisioning of raw materials throughout the alluvial corridor.

## 5. Conclusions

The geomorphological connection between the Guadaíra and Guadalquivir Rivers creates a structural (landscape units) and functional (terraces, colluvial sediments, and floodplains) connectivity. This double connectivity favored hominid dispersal and the apparition of archaeological sites with diverse functionality. A total of 20 archaeological sites (28 assemblages) were studied, with industries from the Guadalquivir, Guadaíra, and Rozalejo Rivers' alluvial sediments, Sierra de Esparteros piedmont's karstic fillings (Cerro Santisteban), colluvial deposits (Rozalejo and La Liebre), and the geomorphological surface. Altogether, 13,233 lithic pieces were analyzed. The chronology of the archaeological sites is Middle Paleolithic (MIS6/MIS5–MIS3), with industries of quartzite and flint coming from, respectively, Sierra Morena–Paleozoic and Subbetic or Mesozoic–Betic. The lithic pieces' features, provenance, transport, and use–wear designed a geoarchaeological hominid alluvial corridor (HAC), underlining two features:

1. The dispersion and geographical density of the archaeological sites throughout the study area of this study prove hominids moved during the Middle–Upper Pleistocene. The archaeological sites' locations in the alluvial series of terraces, as well as on their surfaces, illustrate as much of an occupation of the valleys' bottoms as of the highest terraces of the watersheds. We have characterized this geographical unity as the Guadaíra–Guadalquivir hominid alluvial corridor (HAC). It behaved as a multifunctional corridor, with three leading types of defined activities and another undefined (indeterminate site): food gathering and the distribution of raw materials (habitual or recurrent site and temporary site) and lithic knapping (lithic workshop site). Moreover, this research proposes, since an HAC has been identified, to manage its natural and cultural heritage as a protected geoarchaeological landscape.
2. Two episodes with different durations have been identified: The first one, of short duration, occurred during the Late Middle Pleistocene and Early Upper Pleistocene (MIS6/MIS5) (>129 ka BP and <104 ka BP), and is characterized by notches, scrapers, and knapped pebbles, indicating the persistence of an archaic substratum. The second episode, which lasted much longer, took place during the Upper Pleistocene (MIS3) (<110 ka BP and possibly as recently as 50 ka BP). This episode showcases a wide diversity of flake tools, the presence of the Levallois technique, and bifacial tools.

**Author Contributions:** F.D.d.O.: conceptualization, field work, methodology, writing—original draft, figure preparation, review and editing; J.A.C.G.: conceptualization, field work, methodology, writing—original draft, figure preparation, review and editing; C.B.B.: field work, review, data curation, figure preparation, collection of the sample material; J.M.R.E.: field work, review, data curation, collection of the sample material, pedosedimentological research, laboratory work; R.C.A.: review, data curation, figure preparation; A.M.A.: review, data interpretation, analysis of the U/Th dates. All authors have read and agreed to the published version of the manuscript.

**Funding:** This work received support from the University of Córdoba (Bridging grants for the development of Pre-competitive I+D Projects of the XXII Own Program for the Promotion of Research) and the University of Seville, as well as from the Spanish government (grants for carrying out research projects from the Ministry of Science and Innovation) through public research project funding initiatives.

**Data Availability Statement:** Not applicable.

**Acknowledgments:** This article is a contribution to the research projects GeoCroQ (HAR2011-23798) and DIVERSO (PID2019-103987GB-C33). Research Group PAIDI RNM273, Cuaternario y Geomorfología. The authors would like to express their gratitude to Carmen Pacheco Rubio from the University of Seville for her valuable collaboration in composing this article and engaging in discussions.

**Conflicts of Interest:** The authors declare no conflict of interest.

## References

1. Wohl, E.; Brierley, G.; Cadol, D.; Coulthard, T.J.; Covino, T.; Fryirs, K.A.; Grant, G.; Hilton, R.G.; Lane, S.N.; Magilligan, F.J.; et al. Connectivity as an emergent property of geomorphic systems. *Earth Surf. Process. Landf.* **2019**, *44*, 4–26. [CrossRef]
2. Lexartza-Artza, I.; Wainwright, J. Hydrological connectivity: Linking concepts with practical implications. *Catena* **2009**, *79*, 146–152. [CrossRef]
3. Fremier, A.K.; Seo, J.I.; Nakamura, F. Watershed controls on the export of large wood from stream corridors. *Geomorphology* **2010**, *117*, 33–43. [CrossRef]
4. Bracken, L.J.; Wainwright, J.; Ali, G.A.; Tetzlaff, D.; Smith, M.W.; Reaney, S.M.; Roy, A.G. Concepts of Hydrological Connectivity: Research Approaches, Pathways and Future Agendas. *Earth-Sci. Rev.* **2013**, *119*, 17–34. [CrossRef]
5. Sánchez-Hernández, C.; Gourichon, L.; Blasco, R.; Carbonell, E.; Chacón, G.; Galván, B.; Hernández-Gómez, C.M.; Rosell, J.; Saladié, P.; Soler, J.; et al. High-resolution Neanderthal settlements in mediterranean Iberian Peninsula: A matter of altitude? *Quat. Sci. Rev.* **2020**, *247*, 106523. [CrossRef]
6. Melchionna, M.; Di Febbraro, M.; Carotenuto, F.; Rook, L.; Mondanaro, A.; Castiglione, S.; Serio, C.; Vero, A.V.; Tesone, G.; Piccolo, M.; et al. Fragmentation of Neanderthals' pre-extinction distribution by climate change. *Palaeogeogr. Palaeoclimatol. Palaeoecol.* **2018**, *496*, 146–154. [CrossRef]
7. Cano, J.A.; Aguirre, E.; Giles, F.; Gracia, J.; Santiago, A.; Mata, E.; Gutiérrez, J.M.; Díaz del Olmo, F.; Baena, R.; Borja, F. Evolución del Pleistoceno en la Cuenca Baja del Miño, Sector La Guardia-Tuy. Secuencia de los Primeros Poblamientos Humanos y Registro Arqueológico. In *Cuaternario Ibérico*; Rodríguez Vidal, J., Ed.; AEQUA: Sevilla, Spain, 1997; pp. 201–212.
8. Browne, C.L.; Wilson, L. Resource selection of lithic raw materials in the Middle Paleolithic. *J. Hum. Evol.* **2011**, *61*, 597–608. [CrossRef]
9. Bruxelles, L.; Jarry, M. Climatic conditions, settlement patterns and cultures in the Paleolithic: The example of the Garonne Valley (southwest France). *J. Hum. Evol.* **2011**, *61*, 538–548. [CrossRef]
10. Moncel, M.H.; Moigne, A.M.; Comber, J. Towards the Middle Palaeolithic in Western Europe: The case of Orgnac 3 (southeastern France). *J. Hum. Evol.* **2012**, *63*, 653–666. [CrossRef]
11. Turq, A.; Roebroeks, W.; Bourguignon, L.; Faivre, J.P. The fragmented character of Middle Palaeolithic stone tool technology. *J. Hum. Evol.* **2013**, *65*, 641–655. Available online: <https://www.sciencedirect.com/science/article/pii/S0047248413001899> (accessed on 30 January 2021). [CrossRef]
12. Fitzsimmons, K.E.; Iovita, R.; Sprafke, T.; Glantz, M.; Talamo, S.; Horton, K.; Beeton, T.; Alipova, S.; Bekseitov, G.; Ospanov, Y.; et al. A chronological framework connecting the early Upper Palaeolithic across the Central Asian piedmont. *J. Hum. Evol.* **2017**, *113*, 107–126. [CrossRef] [PubMed]
13. Méndez-Quintas, E.; Santonja, M.; Pérez-González, A.; Arnold, J.; Demuro, M.; Duval, M. A multidisciplinary overview of the Lower Mino River Terrace 1 system (NW Iberian Peninsula). *Quat. Int.* **2020**, *566–567*, 57–77. [CrossRef]
14. Díaz del Olmo, F.; Vallespí, E.; Baena, R.; Recio, J.M. Terrazas Pleistocenas del Guadalquivir Occidental: Geomorfología, Suelos, Paleosuelos y Secuencia Cultural. In *El Cuaternario en Andalucía Occidental*; AEQUA: Sevilla, Spain, 1989.
15. Baena, R.; Díaz del Olmo, F. Cuaternario aluvial de la depresión del Guadalquivir: Episodios geomorfológicos y cronología paleomagnética. *Geogaceta* **1994**, *15*, 102–103.
16. Vallespí, E. Las industrias achelenses en Andalucía: Ordenación y comentarios. *Spal* **1992**, *1*, 61–78. [CrossRef]
17. Vallespí, E. Comentario al Paleolítico Ibérico: Continuidad, etapas y perduraciones del proceso tecnocultural. *Spal* **1999**, *9*, 39–46. [CrossRef]
18. Bridgland, D.R.; Antoine, P.; Limondin-Lozouet, N.; Santisteban, J.I.; Westaway, R.; White, M.J. The Palaeolithic occupation of Europe as revealed by evidence from the rivers: Data from IGCP 449. *J. Quat. Sci.* **2006**, *21*, 437–455. Available online: <https://onlinelibrary.wiley.com/doi/abs/10.1002/jqs.1042> (accessed on 5 February 2021). [CrossRef]
19. Vallespí, E.; Fernández, J.J.; Caro, J.A. Las claves secuenciales del Paleolítico Inferior de Andalucía. *Caesaraugusta* **2007**, *78*, 69–72.
20. Caro, J.A. Evolución de Las Industrias Achelenses en Las Terrazas Fluviales del Bajo Guadalquivir (780.000–40.000 B.P.): Episodios Geomorfológicos y Secuencia paleolítica. *Spal* **2000**, *9*, 189–207. Available online: <https://dialnet.unirioja.es/servlet/articulo?codigo=625246> (accessed on 5 February 2021). [CrossRef]
21. Caro, J.A. Yacimientos e Industrias Achelenses en Las Terrazas Fluviales de la Depresión del Bajo Guadalquivir (Andalucía, España). Secuencia Estratigráfica, caracterización Tecnocultural y Cronología. *Carel Carmona Rev. Estud. Locales* **2006**, *4*, 1423–1605. Available online: [https://www.academia.edu/16632019/Yacimientos\\_e\\_industrias\\_achelenses\\_en\\_las\\_terrazas\\_fluviales\\_de\\_la\\_depresi%C3%B3n\\_del\\_bajo\\_Guadalquivir\\_Andaluc%C3%A0a\\_Espa%C3%B1a.\\_.Secuencia\\_estratigr%C3%A1fica\\_caracterizaci%C3%B3n\\_tecnocultural\\_y\\_cronolog%C3%A0a](https://www.academia.edu/16632019/Yacimientos_e_industrias_achelenses_en_las_terrazas_fluviales_de_la_depresi%C3%B3n_del_bajo_Guadalquivir_Andaluc%C3%A0a_Espa%C3%B1a._.Secuencia_estratigr%C3%A1fica_caracterizaci%C3%B3n_tecnocultural_y_cronolog%C3%A0a) (accessed on 5 February 2021).

22. Caro, J.A.; Díaz del Olmo, F.; Cámara, R.; Recio, J.M.; Borja, C. Geoarchaeological alluvial terrace system in Tarazona: Chronostratigraphical transition of Mode 2 to Mode 3 during the middle-upper pleistocene in the Guadalquivir River valley (Seville, Spain). *Quat. Int.* **2011**, *243*, 143–160. [[CrossRef](#)]
23. Caro, J.A.; Díaz del Olmo, F.; Barba, L.; Garrido, J.M.; Borja, C.; Recio, J.M. Paleolítico Medio Antiguo del valle del Guadalquivir: Las industrias de pequeñas lascas del yacimiento de Tarazona III (Sevilla, España). *Spal* **2021**, *30.1*, 9–45. [[CrossRef](#)]
24. Baena, R.; Fernández, J.J.; Guerrero, I.C.; Posada, J.C. La Terraza Compleja del río Guadalquivir en “Las Jarillas” (La Rinconada, Sevilla. SW de España): Cronoestratigrafía, industria lítica y macro-fauna asociada. *Cuatern. Geomorfol.* **2014**, *28*, 107–125.
25. Díaz del Olmo, F.; Vallespí, E.; Baena, R. Bajo Guadalquivir y Afluentes Secundarios: Terrazas Fluviales y Secuencia Paleolítica. In *Anuario Arqueológico de Andalucía. Actividades Sistemáticas 1990*; Junta de Andalucía: Sevilla, Spain, 1993; pp. 35–39.
26. Soil Survey England and Wales. *Soil Survey Laboratory Methods*; Technical monographs; Rothamsted Experimental Station: Harpenden, UK, 1974; 83p.
27. Duchaufour, P. *Manual de Edafología*; Masson, T., Ed.; Publisher: Barcelona, Spain, 1975; 476p.
28. Munsell Color. *Munsell Soil Color Chart*; Koll Morgen Instruments Corporation: Trapelo Road Waltham, MA, USA, 1990.
29. Bordes, F. *Typologie du Paléolithique Ancien et Moyen*; DELMAS, Ed.; Publisher: Bordeaux, France, 1961; Volume 2, p. 108.
30. Tixier, J. *Les Hacheraux dans L’Acheléen Nord-Africain. Notes Typologiques*; Etrait du congrés Préhistorique du France. Comptere due de la XV<sup>a</sup> sossión Poitiers-Angouleme 15-22 juillet; Société Préhistorique Française: Paris, France, 1956.
31. Clark, G. *World Prehistory in New Perspective*; Cambridge University Press: Cambridge, UK, 1977.
32. Boëda, E.; Geneste, J.M.; Meignen, L. Identification de chaînes opératoires lithiques du Paléolithique ancien et moyen. *Paléo* **1990**, *2*, 43–80. [[CrossRef](#)]
33. Boëda, E.; Kervazo, B.; Mercier, N.; Valladas, H. Barbas C’3 base (Dordogne). Une industrie bifaciale contemporaine des industries du Moustérien ancien: Une variabilité attendue. *Quat. Nova* **1996**, *VI*, 465–504.
34. Caro, J.A. Los Triedros del Yacimiento Achelense de El Caudal (Carmona, Sevilla): Ensayo de una Clasificación Tecnomorfológica. In *Cuaternario Ibérico*; Rodríguez Vidal, J., Ed.; AEQUA: Huelva, Spain, 1997; pp. 322–325.
35. Santonja, M.; Pérez-González, A. (Eds.). *Las Industrias Paleolíticas de La Maya I en su Ámbito Regional*; Excavaciones Arqueológicas en España; Ministerio de Cultura: Madrid, Spain, 1984; Volume 135.
36. Boëda, E. Le débitage discoïde et le débitage Levallois récurrent centripète. *Bull. Société Préhistorique Française* **1993**, *90*, 340–392. [[CrossRef](#)]
37. Boëda, E. Determination des Unités Techno-Fonctionnelles de Pièces Bifaciales Provenant de la Couche Acheuléenne C’3 Base du Site de Barbas I. In *Les Industries à Outils Bifaciaux du Paléolithique Moyen d’Europe Occidentale*; Cliquet, D., Ed.; ERAUL 98: Liège, Belgium, 2001; pp. 51–75.
38. Inizan, M.L.; Reduron, M.; Roche, H.; Tixier, J. *Technologie de la Pierre Taillée. Préhistoire de la Pierre Taillée 4*; Cercle de Recherches et d’Etudes Préhistoriques (CREPS)/Centre National de la Recherche Scientifique (C.N.R.S.): Paris, France; Meudon, France, 1995.
39. Carbonell, E.; Mosquera, M.; Ollé, A.; Rodríguez, X.P.; Sahnouni, M.; Sala, R.; Vergès, J.M. Structure morphotechnique de l’industrie lithique du Pléistocène inférieur et moyen d’Atupuerca (Burgos, Espagne). *L’anthropologie* **2001**, *105*, 259–280. [[CrossRef](#)]
40. Turq, A. Réflexions sur le Biface Dans Quelques Sites du Paléolithique Ancien-Moyen en Grotte ou Abri du Nord-Est du Bassin Aquitain. In *Les Industries à Outils Bifaciaux du Paléolithique Moyen d’Europe Occidentale*; Cliquet, D., Ed.; ERAUL 98: Liège, Belgium, 2001; pp. 141–149.
41. Bourguignon, L.; Faivre, J.P.; Turq, A. Ramification des chaînes opératoires: Une spécificité du Moustérien? *Paleo* **2004**, *16*, 37–48.
42. Geribàs, N.; Mosquera, M.; Vergès, J.M. What novice knappers have to learn to become expert stone toolmakers. *J. Archaeol. Sci.* **2010**, *37*, 2857–2870. [[CrossRef](#)]
43. Soressi, M.; Geneste, J.M. The History and Efficacy of the Chaîne Opératoire Approach to Lithic Analysis: Studying Techniques to Reveal Past Societies in an Evolutionary Perspective. *Paleoanthropology* **2011**, 334–350. [[CrossRef](#)]
44. Pelegrin, J. Las Experimentaciones Aplicadas a la Tecnología Lítica. In *La Investigación Experimental Aplicada a la Arqueología*; Morgado, A., Baena, J., García, D., Eds.; Universidad de Granada: Granada, Spain, 2013; pp. 31–35.
45. Gibaja, J.F.; Clemente, I.; Mir, A. Análisis Funcional en Instrumentos de Cuarzita: El Yacimiento del Paleolítico Superior de la Cueva de la Fuente del Trucho (Colungo, Huesca). In *Análisis Funcional. Su Aplicación al Estudio de Sociedades Prehistóricas*; Clemente, I., Risch, R., Gibaja, J.F., Eds.; British Archaeological Reports, International Series; Hadrian Books Ltd.: Oxford, UK, 2002; Volume 1073, pp. 253–264.
46. Reynard, J.; Henshilwood, C.S. Subsistence strategies during the later Middle Stone Age in the southern Cape of South Africa: Comparing the Still Bay of Blombos Cave with the Howiesons Poort of Klipdrift Shelter. *J. Hum. Evol.* **2017**, *108*, 110–130. [[CrossRef](#)]
47. Venditti, F.; Nunziante-Cesaro, S.; Parush, Y.; Gopher, A.; Barkai, R. Recycling for a purpose in the late Lower Paleolithic Levant: Use-wear and residue analyses of small sharp flint items indicate a planned and integrated subsistence behavior at Qesem Cave (Israel). *J. Hum. Evol.* **2019**, *131*, 109–128. [[CrossRef](#)]
48. Smith, G.M.; Ruebens, K.; Gaudzinski-Windheuser, S.; Steele, T.E. Subsistence strategies throughout the African Middle Pleistocene: Faunal evidence for behavioral change and continuity across the Earlier to Middle Stone Age transition. *J. Hum. Evol.* **2019**, *127*, 1–20. [[CrossRef](#)]
49. Zimmerman, D.W. Thermoluminescence Dating Using Fine Grain from Pottery. *Archaeometry* **1971**, *13*, 29–52. [[CrossRef](#)]
50. Fleming, S.J. Thermoluminescence Dating Refinement of Quartz Inclusion Method. *Archaeometry* **1970**, *12*, 13–30. [[CrossRef](#)]
51. Nambi, K.S.V.; Aitken, M.J. Annual dose conversion factors for TL and ESR dating. *Archaeometry* **1986**, *28*, 202–205. [[CrossRef](#)]

52. Aitken, M.J. *TL Dating*; Academy Press: London, UK, 1985.
53. Arribas, J.G.; Millán, A.; Sibilia, E.; Calderón, T. Factores que afectan a la determinación del error asociado a la datación absoluta por TL: Fabrica de ladrillos. *Bol. Soc. Es. Min.* **1990**, *13*, 141–147.
54. Fernández Caro, J.J. El musteriense clásico de la paleocavidad del cerro de Santisteban (Morón de la Frontera, Sevilla). *Spal* **2003**, *12*, 53–80. [[CrossRef](#)]
55. Baena, J.; Polo, J.; Báñez, S.; Cuartero, F.; Roca, M.; Lázaro, A.; Nebot, A.; Pérez-González, A.; Pérez, T.; Rus, I.; et al. Tecnología musteriense en la región madrileña: Un discurso enfrentado entre valles y páramos de la Meseta sur. *Treb. D'arqueologia* **2008**, *14*, 249–278.
56. Eixea, A.; Villaverde, V.; Zilhão, J. Aproximación al aprovisionamiento de materias primas líticas en el yacimiento del Paleolítico medio del Abrigo de la Quebrada (Chelva, Valencia). *Trab. Prehist.* **2011**, *68*, 65–78. [[CrossRef](#)]
57. Fontana, F.; Moncel, M.H.; Nenzioni, G.; Onorevoli, G.; Peretto, C.; Combier, J. Widespread diffusion of technical innovations around 300,000 years ago in Europe as a reflection of anthropological and social transformations? New comparative data from the western Mediterranean sites of Orgnac (France) and Cave dall'Olio (Italy). *J. Anthropol. Archaeol.* **2013**, *32*, 478–498. [[CrossRef](#)]
58. Goval, E.; Herisson, D.; Locht, J.L.; Coudenneau, A. Levallois points and triangular flakes during the Middle Palaeolithic in northwestern Europe: Considerations on the status of these pieces in the Neanderthal hunting toolkit in northern France. *Quat. Int.* **2016**, *411*, 216–232. [[CrossRef](#)]
59. Meignen, L.; Bar-Yosef, O. Acheulo-Yabrudian and Early Middle Paleolithic at Hayonim Cave (Western Galilee, Israel): Continuity or break? *J. Hum. Evol.* **2020**, *139*, 102733. [[CrossRef](#)]
60. Richards, M.P.; Trinkaus, E. Isotopic evidence for the diets of European Neandertals and early modern humans. *Proc. Natl. Acad. Sci. USA* **2009**, *106*, 16034–16039. Available online: [http://refhub.elsevier.com/S0305-4403\(15\)00113-2/sref48](http://refhub.elsevier.com/S0305-4403(15)00113-2/sref48) (accessed on 28 November 2021). [[CrossRef](#)]
61. Rots, V. Insights into early Middle Palaeolithic tool use and hafting in Western Europe. The functional analysis of level IIa of the early Middle Palaeolithic site of Biache-Saint-Vaast (France). *J. Archaeol. Sci.* **2013**, *40*, 497–506. [[CrossRef](#)]
62. Ruebens, K. Regional behaviour among late Neanderthal groups in Western Europe: A comparative assessment of late Middle Palaeolithic bifacial tool variability. *J. Hum. Evol.* **2013**, *65*, 341–362. [[CrossRef](#)] [[PubMed](#)]
63. Amick, D.S. The recycling of material culture today and during the Paleolithic. *Quat. Int.* **2015**, *361*, 4–20. [[CrossRef](#)]
64. Díez, C.; Alonso, R.; Bengoechea, A.; Colina, A.; Jordé, F.J.; Navazo, M.; Ortiz, J.E.; Pérez, S.; Torres, T. El Paleolítico Medio en el valle del Arlanza (Burgos). Los sitios de la Ermita, Millán y la Mina. *Cuatern. Geomorfol.* **2008**, *22*, 135–157. Available online: [http://tierra.rediris.es/CuaternarioyGeomorfologia/images/vol22\\_3\\_4/08\\_Diez%20Alonso.pdf](http://tierra.rediris.es/CuaternarioyGeomorfologia/images/vol22_3_4/08_Diez%20Alonso.pdf) (accessed on 27 November 2021).
65. Baena, J.; Ortiz, I.; Torres, C.; Báñez, S. Recycling in abundance: Re-use and recycling processes in the Lower and Middle Paleolithic contexts of the central Iberian peninsula. *Quat. Int.* **2015**, *361*, 142–154. [[CrossRef](#)]
66. Jordá, J.F.; Baena, F.; Cabral, P.; García-Guinea, J.; Correcher, V.; Yravedra, J. Procesos sedimentarios y diagenéticos en el registro arqueológico del yacimiento pleistoceno de la cueva de El Esquilleu (Picos de Europa, norte de España). *Cuatern. Geomorfología* **2008**, *22*, 31–46. Available online: [http://tierra.rediris.es/CuaternarioyGeomorfologia/images/vol22\\_3\\_4/02\\_Jorda%20Baena.pdf](http://tierra.rediris.es/CuaternarioyGeomorfologia/images/vol22_3_4/02_Jorda%20Baena.pdf) (accessed on 26 March 2022).
67. Cuartero, F.; Alcaraz-Castaño, M.; López-Recio, M.; Carrión-Santafé, E.; Baena-Preysler, J. Recycling economy in the Mousterian of the Iberian Peninsula: The case of study of El Esquilleu. *Quat. Int.* **2015**, *361*, 113–130. [[CrossRef](#)]
68. Lemorini, C.; Stiner, M.C.; Gopher, A.; Shimelmitz, R.; Barkai, R. Use-wear analysis of an Amudian laminar assemblage from the Acheuleo-Yabrudian of Qesem Cave, Israel. *J. Archaeol. Sci.* **2006**, *33*, 921–934. [[CrossRef](#)]
69. Viallet, C. Macrotraces of Middle Pleistocene bifaces from two Mediterranean sites: Structural and functional analysis. *Quat. Int.* **2016**, *411*, 202–211. [[CrossRef](#)]
70. Agam, A.; Zupancich, A. Interpreting the Quina and demi-Quina scrapers from Acheulo-Yabrudian Qesem Cave, Israel: Results of raw materials and functional analyses. *J. Hum. Evol.* **2020**, *144*, 102798. [[CrossRef](#)] [[PubMed](#)]
71. Ramos-Muñoz, J.; Bernal-Casasola, D.; Barrena-Tocino, A.; Domínguez-Bella, S.; Clemente-Conte, I.; Vijande-Vile, E.; Cantillo-Duarte, J.J.; Almisas-Cruz, S. Middle Palaeolithic Mode 3 lithic technology in the rock-shelter of Benzú (North Africa) and its immediate environmental relationships. *Quat. Int.* **2016**, *413*, 21–35. [[CrossRef](#)]
72. Antoine, P.; Coutard, S.; Guerin, G.; Deschodt, L.; Goval, E.; Locht, J.-L. Upper Pleistocene loess-palaeosols records from Northern France in the European context: Environmental background and dating of the Middle Palaeolithic. *Quat. Int.* **2016**, *411*, 4–24. [[CrossRef](#)]
73. Hérisson, D.; Brenet, M.; Cliquet, D.; Moncel, M.H.; Richter, J.; Scott, B.; Van Baelen, A.; Di Modica, K.; De Loecker, D.; Ashton, N.; et al. The emergence of the Middle Palaeolithic in northwestern Europe and its southern fringes. *Quat. Int.* **2016**, *411*, 233–283. [[CrossRef](#)]

**Disclaimer/Publisher's Note:** The statements, opinions and data contained in all publications are solely those of the individual author(s) and contributor(s) and not of MDPI and/or the editor(s). MDPI and/or the editor(s) disclaim responsibility for any injury to people or property resulting from any ideas, methods, instructions or products referred to in the content.